Strickson, E, Hutchinson, J, Wilkinson, D and Falkingham, P

Can Skeletal Surface Area Predict in vivo Foot Surface Area?

http://researchonline.ljmu.ac.uk/id/eprint/11272/

Article

Can Skeletal Surface Area Predict *in vivo* Foot Surface Area?

E. Catherine Strickson[1], John R. Hutchinson[2], David M. Wilkinson[3] and Peter L. Falkingham[1]

[1]School of Natural Sciences and Psychology, Faculty of Science, Liverpool John Moores University, Liverpool, United Kingdom.

[2]Structure and Motion Laboratory, Department of Comparative Biomedical Sciences, The Royal Veterinary College, Hatfield, United Kingdom.

[3]School of Life Sciences, College of Science, University of Lincoln, Lincoln, United Kingdom.

Corresponding Author:

E. Catherine Strickson[1]

Email address: e.strickson@2016.ljmu.ac.uk

Abstract

The surface area of feet in contact with the ground is a key morphological feature that influences animal locomotion. Underfoot pressures (and consequently stresses experienced by the foot), as well as stability of an animal during locomotion, depend on the size and shape of this area. Here we tested whether the area of a skeletal foot could predict *in vivo* soft tissue foot surface area. Computed tomography scans of 29 extant tetrapods (covering mammals, reptiles, birds and amphibians) were used to produce models of both the soft tissues and the bones of their feet. Soft tissue models were oriented to a horizontal plane, and their outlines projected onto a surface to produce two-dimensional silhouettes. Silhouettes of skeletal models were generated either from bones in CT pose or with all autopodial bones aligned to the horizontal plane. Areas of these projections were calculated using alpha shapes (mathematical tight-fitting outline). Under-foot area of soft tissue was approximately 1.67 times that of skeletal tissue area (~2 times for manus, ~1.6 times for pes, if analyzed separately). This relationship between skeletal foot area and soft tissue area, while variable in some of our study taxa, could provide information about the size of the organisms responsible for fossil trackways, suggest what size of tracks might be expected from potential trackmakers known only from skeletal remains, and aid in soft tissue reconstruction of skeletal remains for biomechanical modelling.

Key Words

Locomotion, ichnology, biomechanics, anatomy

Introduction

The surface area of tetrapod autopodia (feet) reflects several important biomechanical factors, including body mass (McMahon, 1975), habitat (Blackburn et al., 1999), speed (Segal et al., 2004), and bipedal or quadrupedal locomotory habits (Snyder, 1962). Foot surface area is determined by autopodial morphology and posture (Hildebrand, 1980; Full et al., 2002), and, in conjunction with the body mass and locomotory mode of an animal, determines underfoot pressure (Miller et al., 2008; Michilsens et al., 2009; Panagiotopoulou et al., 2012; Qian et al., 2013; Panagiotopoulou et al., 2016).

For very large animals, such as rhinoceroses and elephants, foot surface area needs to be large, as a method of reducing underfoot pressure and avoiding injury to the foot, as well as avoiding sinking on soft ground (Falkingham et al., 2011a). However, foot contact area does not appear to scale isometrically with mass. Larger animals often have smaller foot contact areas than would be expected, and the relationship between foot contact area and mass differs between unguligrade, digitigrade and plantigrade animals (Michelsens et al., 2009; Chi and Roth, 2010). Large animals must compensate for their size with other mechanisms, such as fatty footpads, in order to reduce stress (Panagiotopoulou et al., 2012). Presumably the extinct sauropod dinosaurs, many times larger than extant elephants (Bates et al., 2016) used similar compensatory adaptations (Platt and Hasiotis, 2006).

Foot surface area is also reflective of an animal’s posture and limb use (Biewener, 1989), with bipedal animals requiring feet large enough to support their body weight with half as many limbs as their quadrupedal counterparts (Gatesy and Biewener, 1991), and, in the case of birds, in a huge range of environments and ecological niches with different demands (Alexander, 2004). An animal's balance (e.g. keeping the body's centre of mass (CoM) close to the centre of pressure of feet-- influenced by foot area) is also of vital importance, as the stability of an animal during locomotion is vital to its ability to catch prey, escape predators, migrate effectively, and avoid injury when overexerting itself and when moving on unstable ground (Hodgins and Raibert, 1991; Patla, 2003; Geyer et al., 2006; Birn-Jeffery et al., 2014).

Foot surface area appears to correlate with relative speed during certain forms of locomotion. Body mass has a direct effect on maximum running speed, especially notable in large animals, as speed scales with body mass up to moderate sizes and then declines (Garland, 1983; Bejan and Marden, 2006), and the duration of foot contact with the ground also scales with body mass (Farley et al., 1993). The position and number of toes also tends to be a specialisation for terrestrial running, with a reduced number of toes present in both horses and ostriches (among other cursorial taxa; Coombs, 1978), reducing foot weight, a useful adaptation because heavier feet necessitate more energy usage to recover from a stride (Snyder, 1962; McGuigan and Wilson, 2003; Schaller, et al., 2011). Peak plantar pressure and speed are demonstrably linked in humans (Rosenbaum et al., 1994; Segal et al., 2004; Pataky et al., 2008) and ostriches (Schaller, et al., 2011); however, this link has not been fully explored in other terrestrial animals, especially quadrupeds.

Large feet have a potentially conflicting relationship with speed in that they will be more massive and thus have greater inertia, making them more difficult to swing quickly through the air (Taylor et al., 1974; Fedak et al., 1982; Kilbourne and Hoffman, 2013; Kilbourne and Carrier, 2016). Nonetheless, it is important that foot surface area and underfoot pressures evolve to allow an organism's locomotion to be energy-efficient and its posture stable, while enabling sufficient bursts of speed if necessary. In other words, the surface area of the autopodia should be subject to selective pressures in the same manner as any other part of the locomotor system.

Foot surface area is also potentially influenced by Allen's rule (Allen, 1877; Allee and Schnidt, 1937), which supposes that warm-blooded animals in cold climates will tend to have smaller feet than their relatives in warmer clines (Blackburn et al., 1999). This may or may not be due to causal links (i.e. natural selection) to either reduce surface area exposed to the cold, or be a reflection of adaptations in warmer climates to increase surface area to promote heat dissipation. This 'rule' may conflict with constraints imposed by keeping pressures low (i.e. foot areas large) to avoid sinking into soft substrates such as snow or sand. Allen's rule also potentially conflicts with the outcome of Bergmann's rule – the contentious but broadly supported tendency for ectotherms to be larger in colder climates (Clarke, 2017). Therefore, colder conditions will tend to correlate with increased body mass, implying a larger foot surface area while simultaneously selecting for smaller feet.

Some animals exhibit notable disparity in the size of fore- and hind-feet, which is apparent in their foot surface area: a condition known as heteropody. A previous study (Henderson, 2006) demonstrated that the ratio of fore- and hind-foot surface areas, in its subject animals, could match CoM position, e.g. an elephant has 40%/60% relative fore- vs. hind-foot surface area, and a CoM of 40% of the distance from the glenoid to the acetabulum. It would seem logical to assume that animals spread their body weight relatively evenly over their feet, in order to reduce maximum pressure, excess tissue or substrate stress and strain (Cheung et al., 2005), and to prevent sinking when walking across compliant substrates

(Falkingham et al., 2011a). However, this assumption runs contrary to pressure experiments showing higher mean peak pressures in elephant forelimbs (Panagiotopoulou et al., 2012). It is therefore worth exploring a possible correlation of the relative sizes of an animal's manus and pes, and CoM with both observations in mind, and worth considering possible implications of such a correlation across Tetrapoda.

Heteropody is a common occurrence in some extinct animals, such as sauropod dinosaurs, as indicated by trace fossil evidence (Lockley et al., 1994; Henderson, 2006). Preserved trackways from these dinosaurs indicate that often their fore- and hind-feet impressions differ in depth (Falkingham et al., 2011b; Falkingham et al., 2012), implying differential underfoot pressures. Determining foot surface area in these animals can be complex, however, and attribution of specific trackmakers to trackways is notoriously difficult (Farlow, 1992; Clack, 1997; Falkingham, 2014a), partly because matching impressions of fully fleshed feet to skeletal remains would require accurate methods of predicting skeletal to skin foot morphology, which is currently difficult and largely speculative (Jannel et al., 2019). Indeed, matching the tracks of extant animals to the correct species is often not straightforward – as illustrated by the existence of field guides produced to help fieldworkers with this problem (e.g. Bang and Dahlstrøm, 2001).

For terrestrial and arboreal fauna, the substrate underfoot can have a noticeable effect on locomotion, and the way the foot moves in a step. Both substrate and autopodial tissue will be compressible to varying degrees, slightly altering foot contact area during stance (Gatesy, et al., 1999; Gatesy, 2003; Falkingham and Gatesy, 2014; Gatesy and Falkingham, 2017).

Palaeobiologists must rely on soft tissue data from extant animals to infer many facets of the morphology of extinct animals (Witmer, 1995), because preservation of soft tissues is rare and only partial details about muscle and tendon structures can be inferred from the skeletal elements they interacted with. In this way, a study of the relationship of flesh and skeletal foot surface area should help to fill gaps in our understanding of the anatomy of extinct animals' feet, as well as the interaction of foot structure and CoM, and would be particularly valuable for linking fossil trackways and supposed trackmakers. Here we aim to test whether skin and skeletal surface area are correlated across Tetrapoda, and if so, if their correlation is strong enough to make it a useful tool in the study of fossils and trackways.

Materials & Methods

In order to compare skeletal and fully fleshed foot anatomy in extant animals, computed tomography (CT) scans of cadaveric autopodia from 29 species of tetrapod (one specimen of each except for *Crocodylus moreletii* and *Osteolaemus teraspis* – see supplementary material), covering amphibians, reptiles, birds, and mammals, were analysed. The sex of individuals was unknown, and all but *Crocodylus niloticus* were adults. All specimens were museum or zoo-donated specimens whose cause of death was unrelated to this study (and generally unknown).

MeVisLab (Heckel et al., 2009) was used to segment the scans into separate 3D models (OBJ format meshes) of the soft tissue and skeletal elements. The resultant meshes were then imported into Autodesk Maya 2018, where they were cleaned, aligned and re-posed to the horizontal plane (figure 1). The aligned meshes were then processed using MatLab (Mathworks Inc. Natick, MA, USA), where they were ‘flattened’ by setting the vertical component of each vertex to 0. This flattening produced 2D ‘silhouettes’ of the models, either as soft tissue of the foot or its skeleton, from which area was calculated using an alpha shape (see below).

Skin models were oriented and posed so that only areas of the feet that would touch the ground during locomotion would be used upon flattening the models, and any parts of the models that extended past this area were removed (figure 1B). The extent of the soles of the feet were, for the most part, obvious from visible anatomy. In addition, from *in vivo* biplanar fluoroscopy studies, X-ray images, and photographs *in situ,* we made educated estimates of accurate positions for taxa (Astley and Roberts, 2014; Bonnan, et al., 2016; Kambic et al., 2015; Panagiotopoulou, et al., 2016). For a more repeatable approach (Pose 2, see below), parts of the skin model extending past the functional foot area (the unguals for unguligrade animals, the digits for digitigrade animals, and the entire sole of the foot for plantigrade animals and semi-digitigrade animals, so that the full extent of fatty foot pads were accounted for) were removed where present.

However, since these models were taken from CT scans, without the full weight of the animal deforming the foot underneath, the true shape of the foot during stance for many of these animals may have been slightly different, due to compliant soft tissues (Alexander, et al., 1986; Gatesy, 2003). This is especially significant for those animals with large fatty foot pads such as *Elephas* and *Ceratotherium*, and less significant for the majority of ungulates, whose hooves are stiff, and more resistant to deformation (Hinterhofer, et al., 2000; Hutchinson, et al., 2011).

Skeletal models were posed in one of two ways. Firstly (Pose 1), matching the pose of skin models (Figure 1B-D), secondly (Pose 2), with all bones aligned to the horizontal (Figure 1E-F). For the latter pose, models were cropped proximal to the digits for digitigrade animals, proximal to the unguals for unguligrade animals, proximal to the tarsals/carpals for plantigrade animals.

For large, semi-digitigrade/subunguligrade animals (*Elephas maximus, Ceratotherium simum*, and *Hippopotamus amphibius*), proximal foot elements are raised off the ground, supported by fatty foot pads, increasing foot contact area. Therefore using only the phalanges, as for other digitigrade animals, would severely underestimate contact area. To explore this ambiguity, skeletal outlines were generated from just the digits (Pose 2a), the digits plus metatarsals (Pose 2b), and with the entire foot skeleton (Pose 2c). This analysis was designed to be more objective and repeatable in determining skin from skeletal surface area, particularly, in extinct animals, where knowledge of *in vivo* foot posture may be lacking.

Results for area where left and right forefeet or hindfeet were available were averaged (mean), as were area results for animals with multiple specimens, and *Camelus,* where both feet were unassigned as forefeet or hindfeet.

It should be noted that our 29 animals studied include several ungulates, possessing large, keratinous hooves, much harder and stiffer than most other tissues categorised under ‘soft tissues’ in this study. While ungulate hooves have properties that distinguish them from other soft tissues, and take longer to decompose than softer tissues, they are also distinct from skeletal tissue, and are rarely preserved, especially in fossils (Pollitt, 2004; Saitta, et al., 2017). In terms of comparisons between skeletal and fossil remains and the overall foot structure of living animals, hooves clearly are an important part of a living ungulate's foot structure, and their ability to locomote; thus being able to predict their size from skeletal remains is as much of a part of the goal of this study as predicting the areas of softer tissues (Warner, et al., 2013). In this sense, the term 'soft tissue' as used in this study refers to 'non-skeletal tissue', with the hardness of these tissues largely irrelevant.

Initially, we attempted to calculate the 2D convex hull (a shape made by joining the outermost data points in a simplified representation of the data (see figure 1C-D, in green)) of each silhouette, but found via pose tests using bird feet that this method was extremely sensitive to pose, particularly whether the digits were laterally spread or not (Supplementary material 1). Instead, 2D, tight-fitting alpha shapes (where the outermost data points were joined in a shape that most closely fits the silhouette's true shape (figure 1C-D, in pink)) were produced for each silhouette, and the area of these alpha shapes calculated. The alphaShape command in MatLab uses an 'alpha value' to determine the maximum distance between edge points to bridge (a sufficiently large 'alpha value' will produce a convex hull). We used the automatically determined alpha value for each alpha shape, which is calculated based on the density of vertices in the model, as this produces the tightest fitting single shape for any given set of points. We set the hole threshold to be extremely large (larger than the foot as a whole) to remove any holes from the interior of the alpha shape. The surface area of the skeleton's alpha shape as a percentage of the skin's shape was then used to compare each organism.

The dataset was then run through PGLS (phylogenetic generalised least squares) regression analyses to assess the significance of the relationship between the variables, and how much impact common ancestry between the animals studied affected the results (Blomberg et al., 2012; Felsenstein, 1985). This was accomplished using Mesquite (Maddison and Maddison, 2001) to draw three simple trees (manually compiled "consensus" phylogenies based on the most recent and broadly accepted phylogenies at the time of writing, within which the placement of Carnivora, Cetartiodactyla and Perissodactyla in relation to each other, was the only major point of contention (Gauthier et al., 1988; Nery et al., 2012; Prum et al., 2015)) connecting the organisms involved in this study. We then applied the Grafen method (Grafen, 1989) of branch length estimation to the trees, and ran PGLS via the Ape (Paradis et al., 2004), Geiger (Harmon et al., 2008), Nlme (Bliese, 2006) and Phytools (Revell, 2012) packages in R. Results for forefeet, hindfeet, and all feet were each tested. The influence of body mass was also tested using PGLS, in order to determine whether phylogeny, body mass, or a combination of both factors had a significant effect on the relationship between skin and skeletal foot surface area. P values <0.05 were considered significant. Body masses were taken from scan metadata where possible, or estimated from the literature (e.g. Dunning Jr, 1992) where such metadata were not available (Supplementary material 1).

Skin surface area was plotted against skeletal surface area for all analyses, using the entire data set, and then broken up into smaller groups: unguligrade, digitigrade, plantigrade, terrestrial, semi-aquatic, erect posture, sprawling posture, mammals, and birds. The plots were framed in terms of the predictability of skeletal area from skin area, to emphasise potential utility for trackmaker identification from fossils. However, these data are intended to be interpretable both ways, and the prediction of *in vivo* surface area from skeletal remains is of equal utility. For the purposes of these analyses, the digitigrade (Pose 2a) and plantigrade (Pose 2c) poses of semi-digitigrade/subunguligrade (*sensu* Carrano, 1997) animals were added to their respective groups, whereas Pose 2b was used for the remaining groups, as it represents an intermediate pose. Semi-aquatic included amphibians, crocodilians and hippopotamuses, terrestrial did not include birds except for *Dromaius novaehollandiae*, and sprawling (here meaning non-erect) posture included amphibians, lepidosaurs and crocodilians, although crocodilians use a range of limb postures spanning the sprawling-to-erect continuum (Gatesy, 1991; Reilly and Elias, 1998).

Results

For the Pose 1 analysis (approximate life position), projected foot skeleton surface area as a percentage of projected fully fleshed foot surface area (Figure 2, above cladogram) was an average of 56% (both mean and median) for all organisms measured (three amphibians, four crocodilians, seven birds, and fourteen mammals), with means of 49% for amphibians (53% median), 47% for crocodilians (48% median), 68% for birds (67% median), and 55% for mammals (54% median) with an average standard deviation of 13%. Extremely similar results were found with bones oriented as in Pose 2. The smallest percentages of skeletal vs. fleshed surface area observed were in *Equus* species (*Equus quagga* at 34%, *Equus ferus caballus* 38%), *Giraffa camelopardalis* (38%), *Crocodylus niloticus* (38%), and *Cryptobranchus alleganiensis* (39%). However, besides *Equus* and *Giraffa*, other ungulates did not stand out as having particularly low skeletal areas relative to skin areas. Carnivorans had proportionately high skeletal calculated area. The highest skeletal areas relative to skin areas (as seen from the underside, and in two dimensions) were *Coturnix coturnix* at 83%, followed by *Panthera leo persica* and *Ceratotherium simum*, at 81% and 73%, respectively.

Where skeletal models were set flat (Pose 2), all unguligrade animals expressed lower skeletal area compared to skin surface area, compared with Pose 1 (Figure 2). The zebra stood out most with just 22% skeletal representation.

Elephas, Hippopotamus, and *Ceratotherium* showed considerable variability depending on which foot bones (Pose a/b/c) were used to predict skeletal area: *Hippopotamus* (37/76/100%), *Ceratotherium* (31/74/98%), *Elephas* (17/42/68%). 100% skeletal surface area representation in the hippopotamus clearly suggests that treating these animals as plantigrade does not yield results representative of these animals' foot morphology, or indeed results that are useful for predictive purposes, especially given the steep (subvertical) angle at which these animals position their feet *in situ*.

Carnivorans, particularly cats, typically do not have their digits extended fully when walking or standing, as such relative skeletal area calculated from Pose 2 (eg. *Panthera* 93%, *Vulpes* 92%) generally produces higher relative skeletal areas than the more life-like Pose 1 (eg. *Panthera* 81%, *Vulpes* 70%).

Overall, mammalian data were highly variable (47% range from maximal to minimal values in Pose 1, over 80% range in Pose 2). Given that mammalian species dominated our study sample (then birds, then crocodilians), perhaps with more data the variability within other groups would increase to comparable levels. However, that mammalian feet have unusually high morphological disparity compared to other taxa in our sample, is reflective of their unusually high morphological disparity in terms of body size, foot anatomy, and posture compared to other groups (Kubo et al., 2019).

Bird and crocodilian data were more consistent than mammals (25% range for birds in all analyses, 18% range for crocodilians). *Dromaius*, which was morphologically and functionally distinct from the other birds in the study in terms of being large and flightless, fell neatly within the range for birds.

Raw numbers for projected skeleton and projected skin surface area, calculated from Pose 1, were plotted as a log graph, and a power trendline fitted (Figure 3). This plot, despite the variation seen in Figure 2, showed a strongly positive correlation ($R^2 = 0.99$, p value <0.05) in 'Pose 1' between skin and skeletal foot surface area. This correlation can be described with the equation $y = 0.59x^{0.99}$ (where y = skeletal foot surface area and x = foot skin surface area). This skin and skeletal foot surface area's scaling relationship was close to isometry (slope of 1.0). Soft tissue surface area may therefore be predicted, on average, as approximately 1.67 times skeletal surface area. There were very few outlying animals, indeed, *Elephas* and *Ceratotherium* were the only animals that diverged notably from the linear trendline. If the three largest animals were removed from the data set, or the three smallest, the strength of the correlation was unaffected, but soft tissue area predictions from skeletal area decreased (Supplementary Material 1). If both groups were removed, the predicted value decreased further.

When the forelimb and hindlimb results were calculated separately, the equations differed noticeably ($y = 0.52x^{0.99}$ and $y = 0.64x^{0.98}$ respectively); although the difference in slope was not statistically significant, and R^2 values remained ~0.99 (Figure 3). However, soft tissue area was ~2 times skeletal area in the forelimb, but only ~1.56 times in the hindlimb. See Table 1 for full list of formulae and R^2 values, rounded to two significant figures (and see Supplementary Material 1 for slope uncertainties for all poses, and for all limbs, forelimbs, and hindlimbs.).

For all flat pose analyses (Pose 2), heavier animals remained the outliers, with *Elephas, Hippopotamus,* and *Ceratotherium* diverging most from the trendline (Figure 4). Similar to the Pose 1 analysis, Pose 2b suggested high predictability, with soft tissue as approximately 1.67 times skeletal surface area. Regressions for Pose 1 and Pose 2b were statistically similar. The analysis treating semi-digitigrade/sub-unguligrade as plantigrade (Pose 2c) suggested soft tissue as approximately 2.04 times skeletal surface area, and semi-digitigrade as digitigrade (Pose 2a) resulted in soft tissue as 1.05 times skeletal surface area. Interestingly, the hindlimbs-only regression for Pose 2b was significantly different from its equivalent with both fore- and hindlimbs and forelimbs-only (Table 1).

PGLS results (e.g. for all feet, in 'Pose 1', with Carnivora and Perissodactyla in a single clade) produced a correlation of -0.171 between the predictor and the intercept, and a Pagel's lambda value ~1, with an adjusted R^2 of 0.92 (t-statistic 18.06, residual S.E. 12005, 29 DF (26 residual)). Similar results were found when running the same tests on fore-and hind-feet separately, with the other two phylogenetic tree arrangements. When skeletal elements were laid flat, variable adjusted R^2, Pagel's lambda (though all ~1), and t-statistics were found, with higher standard error (15686.49 SE (28 DF (26 residual)) in Pose 2a) (Supplementary material 1). Despite these variations, this still suggests that phylogeny is not the main driver of the correlations found.

Separate regressions for unguligrade, digitigrade, plantigrade, terrestrial, semi-aquatic, erect posture, sprawling posture, birds and mammals, all showed strong correlations (Table 2, Supplementary material 1 and 2). Equations for all the analyses varied, with opposing regressions (e.g. sprawling versus erect posture, or terrestrial versus semi-aquatic) statistically different from each other (Table 2, equations and R^2 values rounded to two significant figures). Although R^2 values suggest high correlations for these regressions, the lack of data points in each of them (particularly those with the highest R^2 values) suggests their predictive value is relatively low at present. There are potentially functional reasons why, for example, sprawling animals, semi-aquatic animals, and birds would have stronger correlations and more predictable foot morphologies, but the lower scores in groups with more data points suggests high correlation in groups with few data points may be an artefact, and should be viewed with caution.

Body mass had no significant effect on relative skin/skeletal areas. This was unsurprising because *Ceratotherium* results indicated more skeletal representation than other large animals such as *Elephas*, and percentage of skeletal vs. non-skeletal (skin) area results for small animals did not appear to skew towards either obviously high or low skeletal representation (Supplementary Material 1).

Discussion

Projected skeletal surface area as a percentage of projected skin surface area varied between the organisms studied, most notably in mammals, which yielded both the lowest and second highest values (Figure 2). Bird feet are all similarly digitigrade in their posture and are largely made up of skeleton (with three major digits and consistent phalangeal numbers), skin, and connective tissue, so their more consistent percentages are not surprising considering that some of the mammals in this dataset had hooves, fatty footpads, and a wide range of foot anatomies and postures (from plantigrade to unguligrade). PGLS results suggested that the correlation between skin and skeletal foot surface area in all poses, as well as being very strong, still held with phylogeny taken into account. This suggestion was supported by Figures 3 and 4.

Equus and *Giraffa* stood out in this dataset for having an especially low relative skeletal surface area. All extant horses have one toe with a large, keratinous hoof (Bowker et al., 1998), so this was perhaps to be expected. Giraffes also have relatively small feet and gracile legs compared to other animals of similar size, and a combination of high body mass and high running speeds, which contribute to an overall unique morphology (van Sittert et al., 2015). Pose 2 resulted in a lower relative skeletal area across unguligrade animals, though none as extreme as either *Equus* species. By focusing on ungual bones, it became clear that the keratinous sheath that forms the hoof dominates the 'silhouettes', with skeletal tissue only represented by the very tip of the toe, so this is to be expected. Non-unguligrade ungulates: *Ceratotherium, Hippopotamus*, *Camelus dromedaries, and Vicugna pacos*, did not yield similar results to unguligrade ungulates, and varied significantly from this group, as well as from each other.

For *Crocodylus niloticus*, the fact that Crocodylia have relatively thin, long, digital bones, somewhat similar to human phalanges, that converge to form a surprisingly robust foot, could have some effect (Ferraro and Binetti, 2014). Furthermore, joint range of motion studies have suggested an unusual wrist function and resultant manus posture in crocodilians favouring rigidity, which could affect potential foot contact area (Hutson and Hutson, 2014). This rigidity could potentially aid in swimming, with the stiff foot acting in a flipper-like fashion to push through water efficiently, which smaller crocodilians tend to rely upon (Seebacher, et al., 2003). Furthermore, the *Crocodylus niloticus* specimen used was the only juvenile in this study, and its phalanges were small and spaced far apart in some cases, so this result could be an artefact of ontogeny, or the quality of the models used. Further studies on the effect of ontogeny on skeleton to skin surface area ratio could elucidate this further. Indeed, in future studies consideration should be given to levels of ossification of manus and pes bones. For example, our *Cryptobranchus* CT scan was missing wrist bones on all feet when segmented because these elements were cartilaginous in the specimen scanned, and were indistinguishable from soft tissue. Such ossification is likely to vary across species, and across ontogeny.

At the other extreme, where skeletal surface area was high (most closely approaching projected skin surface area), several birds (most notably *Coturnix*, *Accipiter nisus*, and *Alectoris chukar*) along with carnivorans and *Ceratotherium* (as well as *Hippopotamus* in Pose 2b and 2c) stand out the most. For birds, this is understandable considering their relative lack of musculature and fat in their feet. For carnivorans this could be explained by their claws, extending beyond the main body of the foot, by the resting position of their digits *in vivo,* and by their footpads, for which stiffness scales directly with body mass, while foot contact area lags behind (Chi and Roth, 2010). This scaling allows carnivorans to maintain relatively small feet that are light enough to be moved quickly (Kilbourne and Carrier, 2016; Kilbourne and Hoffman, 2013).

Body mass seemed to have little general effect on the relationship between skin and skeletal foot surface area. Previous studies have found a scaling relationship between body mass and foot contact area not significantly different from isometry (Michilsens et al., 2009), implying that the ratio of skeleton to soft tissue in the foot was not affected by this scaling effect. The scaling relationship between the ratio of skin to skeletal foot surface area was at best trivially different from isometry– a sensible result given that the variables are two facets of the same structure (i.e. the manus or pes), and therefore their structure and development are intrinsically linked. Despite this result, the largest animals in our dataset were the most outlying (much less so when plotted logarithmically (Figure 3)). It is notable that these largest animals, namely, *Elephas, Ceratotherium,* and *Hippopotamus*, were also the only semi-digitigrade/subunguligrade animals in our data. These animals both had the largest feet in the study and possess fatty foot pads to reduce loads on their individual toes and spread out underfoot pressure due to their large body masses (Hutchinson et al., 2011; Regnault et al., 2013). The divergence of these data appears to be influenced by their foot posture as well as their large size, with the adaptation of a semi-digitigrade posture potentially occurring specifically to support their large body weights.

It may be worth considering that beyond a certain weight threshold, specialised foot morphologies are necessary for weight support and locomotion, and thus successively heavier animals may have more disparate soft tissue structure and foot posture adaptations to cope with increased load (Hutchinson, et al., 2011). This has implications for the inherent predictability of our methods for very large extinct animals, such as sauropod dinosaurs, especially where foot posture is loosely inferred and little information about soft tissue structure is available. Follow-up studies on semi-digitigrade foot postures and how they support loads differently to other foot postures, as well as similar studies to this, using additional heavy and semi-digitigrade animals, would increase understanding of this variation of foot form and function. Contrary to the semi-digitigrade animals in our study, the giraffe, an unguligrade animal, was the largest other tetrapod (<1500kg vs. 3000+kg in larger individuals of the semi-unguligrade taxa), and deviated little from trendlines.

The strength of the correlation between skin and skeletal foot surface area, despite variations seen in Figure 2, implied sufficient reliability to predict one from the other (Figure 3).. Despite this, birds only appeared above the trendline (Figure 3). Perhaps a more accurate correlation could be achieved for birds alone with a larger avian dataset (with a wider range of foot sizes), which would allow more accurate predictions of bird foot surface area, and of foot surface area for animals with similar pedal anatomy to birds (such as non-avian theropod dinosaurs). Although our main results could be refined with a much larger tetrapod data set, it appears that foot surface area can be predicted from foot skeletal surface area, with soft tissue generally predictable as approximately 1.67 times skeletal foot surface area, as demonstrated in Poses 1 and 2b. However, when analyzed separately, manus and pes presented differing ratios, with soft tissue surface area of the former being predicted as ~2 times skeletal area, but just ~1.56 times for the pes. This correlation could potentially be used to estimate skeletal foot surface area of animals from their footprints, and its inverse used to predict skin-on-foot surface area of extinct animals from their skeletons, and even of cadavers from skeletons, with potential forensic applications.

For Pose 2, *Elephas, Ceratotherium,* and *Hippopotamus* were tested in three different poses. Their foot anatomy is unusual in that they have a foot posture with most foot elements far off the ground, but also have fatty pads which give them a large foot surface area. With this in mind, all foot elements being in line with the horizontal plane, as in Pose 2c, is highly unrealistic. Pose 2a is perhaps more realistic than 2c, but assumes fewer foot elements are supportive during stance than is accurate *in vivo*. The most representative position for semi-digitigrade would arguably be Pose 1, as this did not force these animals into an unrealistic foot posture. However, both Pose 1, and Pose 2b both result in the same 1.67 times skeletal surface area value, and Pose 2b's intermediate nature tests a pose in between digitigrade and plantigrade. Pose 2b then, is perhaps the best repeatable method. If, despite this, our other methods were chosen to predict foot surface area, skin surface area would be equal to 1.05 times skeletal surface area for Pose 2a, and 2.04 times skeletal surface area for Pose 2c. The variability in these analyses does reveal that altering the results of the largest animals in the study alters the equation used. Therefore, perhaps this method would be best applied to smaller and non-semi-digitigrade animals. However, variation in area results is to be expected when fundamentally changing the number of skeletal elements in an analysis.

Where data were divided into smaller groups for analysis, strong correlations were found in results for plantigrade animals, semi-aquatic animals, sprawling posture, and birds (Table 2). Selective pressures potentially could drive a need for similar foot anatomy across these groups, and therefore predictable foot structures, such as adaptations for perching, swimming, and supporting body weight when feet are not directly under the body. Yet considering that these groups were also the groups with the fewest data points, we cannot draw any definitive conclusions from these results.

In terms of methods used, we found that convex hulls are highly sensitive to foot pose, such as the size of inter-digital angles (Supplementary material 1), a result consistent with previous findings (Cholewo and Love, 1999). This could be the cause of wide error margins if these hulls were used for predictive purposes. This is especially relevant in re-posed foot models, where inter-digital angles are manipulated to resemble *in vivo* arrangements, and in animals that have long, thin digits, such as crocodilians. Alpha shapes produced more consistent, 'tight-fitting' outlines for area calculation, a much more accurate measure of the real scope of foot surface area for these models.

Inevitably, models derived from CT scans, such as those we used, ignore certain *in vivo* factors such as foot deformation during contact with the ground. While we attempted to stick closely to the *in situ* positions of feet (Pose 1), and aimed for a more objective iteration of our analysis by laying bones flat to remove subjectivity (Pose 2), deformation is a very difficult issue to control for. Collection of the data needed to account for this would require advanced *in vivo* imaging techniques such as biplanar fluoroscopy (i.e. "XROMM"; Brainerd et al., 2010; Gatesy et al., 2010); however, such techniques remain limited in the size of potential subjects (e.g. Panagiotopoulou et al., 2016) and can be expensive and time-consuming to conduct. Despite this issue, deformation of the foot should generally not be significant enough that it should diminish the usefulness of this study or the predictability of the methods employed here, as even in soft footpads, foot contact area does not maintain constant stress with body mass, and larger body mass can lead to increased foot stiffness (Chi and Roth, 2010). Combining this methodology with XROMM data for elephants and other animals with large, fatty foot pads, however, would be advantageous in determining the overall effect of deformation on the predictability of these methods and on foot surface area in general, as this particular aspect of foot anatomy is the most prone to deformation with body weight, due to its high compliance (Hutchinson, et al., 2011). Overall, CT scans are a reliable resource for studies like these, and their utility in determining foot surface area could potentially contribute to future studies on animal locomotion and posture if used in conjunction with *in vivo* loading, centre of mass and pressure data. However, as in this study, where quality of the models varied, results could potentially be limited by the fidelity of the scans available, and therefore, more scans available for each animal to have the option to pick and choose the most complete and highest quality, as well as more computing power and high-end software, would be a boon to future studies.

Most studies concerning underfoot areas and pressures have focused on humans and other primates. Adaptations for arboreal locomotion have resulted in large functional differences between the forelimb and hindlimb in primates (Schmitt and Hanna, 2004). Such differences, would make them an interesting subject for a follow-up study.

Assigning specific trackmakers to fossilised trackways is a difficult task (Falkingham, 2014b). It is our hope that these results could be used to constrain potential trackmaker identity. However, as an extrapolation from a bivariate plot, with a number of variables unaccounted for such as soft tissue and substrate compliance, the applications of figure 3 and its predictions are currently limited, and such identifications of trackmakers must be undertaken cautiously.

When predicting the skeletal surface area of the feet of extinct animals, and identifying trackmakers, the many complexities of footprint formation must be taken into account. The shape of footprints is determined not only by foot anatomy, but also dynamics of the limbs, and substrate consistency (Falkingham, 2014a; Minter et al., 2007; Padian and Olsen, 1984). Underfoot pressures (Hatala et al., 2013), centre of mass position (Castanera et al., 2013), and style of locomotion (Hatala et al., 2016) all contribute to variations in limb dynamics, and consequently the morphology of a track. Given that foot size and shape is the focus of this study, the findings herein concern matters of critical importance to footprint formation and trackmaker identification, relating as they do to both anatomy and dynamics.

When trying to model footprint formation and dynamics of extinct animals, centre of mass and underfoot pressures of the animals in question are determining factors. When considering these factors, the difference between manus and pes size and pressure is of great importance. Disparity between the cranial and caudal parts of the body is especially notable as previous biomechanical models have often underestimated mass in the cranial half of the body (See discussion in Allen et al., 2009). Simply put, taking into account the differences between soft tissue area in manus and pes could make a notable difference in estimations of underfoot pressures and simulations of footprint formation. As an example, when the skeletal remains of *Plateosaurus engelhardti* feet were laid flat, and their skin areas predicted from alpha hulls, estimated manus skin area was 32% of pes area when using the 1.67 multiplier from combined analyses, and 40% of pes area using the separate multipliers (2 for manus, 1.6 for pes). Using body mass and centre of mass calculations from Allen et al. (2013), these results predicted manus underfoot pressure of 80% pes pressure when combined, and 64% when separate (Supplementary Material 1). This effect should also be considered in the inverse when considering trackmaker anatomy from fossil footprints. In this way, this method is a useful tool to consider in digital reconstruction and trackmaker identification.

Conclusions

The surface areas of the skin of the foot *in situ* and of the foot's skeletal components are strongly correlated and thus should be predictable in terrestrial tetrapods. Skin surface area was approximately 1.67 times that of skeletal surface area (~2 times for manus, ~1.6 times for pes, if analysed separately). This trend was not affected by body mass and showed little evidence of being strongly affected by phylogeny. This predictability has potential in aiding with estimating the size and possible species of trackmakers in the fossil record, both by estimating the size of skeletal feet using footprints, and by estimating foot size, and therefore potential footprint size, from fossil feet.

Acknowledgements

We thank David Blackburn at the Florida Museum of Natural History for provision of frog CT scans, and Ryan Marek and Ikuko Tanaka, and several members of the Structure and Motion Lab for constructive comments. Thanks to Diego Sustiata and two anonymous reviewers for constructive critique and feedback. Thanks to Phylopic.org silhouette providers Steven Traver, T. Michael Keesey, Mattia Manchetti, Yan Wong, B. Kimmel, Jan A. Venter, Herbert H. T. Prins, David A. Balfour, Rob Slotow, Shyamal, and Elisabeth Östman – images used under their respective creative commons licenses.

Author Contributions

Research and analysis was conducted by ECS. Manuscript and figures by ECS, with contributions from PLF, JRH, and DMW. The majority of the CT scans used were provided by JRH. Research was part of a PhD by ECS, supervised by PLF DMW and JRH.

References

Alexander, R. M., 2004. Bipedal animals, and their differences from humans. J. Anat. 204, 321-330.

Alexander, R. M., Bennet, M. B., Ker, R. F., 1986. Mechanical properties and function of the paw pads of some mammals. J. Zool. Lond. 209, 405-419.

Allee, W.C., Schmidt, K., 1937. Ecological animal geography. John Wiley and Sons.

Allen, J.A., 1877. The influence of physical conditions in the genesis of species. Radic. Rev. 1, 108–140.

Allen, V., Bates, K. T., Li, Z., Hutchinson, J. R., 2013. Linking the Evolution of Body Shape and Locomotor Biomechanics in Bird-Line Archosaurs. Nature 497, 104.

Allen, V., Paxton, H., Hitchinson, J. R., 2009. Variation in Centre of Mass Estimates for Extant Sauropsids and Its Importance for Reconstructing Inertial Properties of Extinct Archosaurs. Anat. Rec. 292, 1442-1461.

Astley, H. C., Roberts, T. J., 2014. The mechanics of elastic loading and recoil in anuran jumping. J. Exp. Biol. 217, 4372-4328.

Bates, K.T., Mannion, P.D., Falkingham, P.L., Brusatte, S.L., Hutchinson, J.R., Otero, A., Sellers, W.I., Sullivan, C., Stevens, K.A., Allen, V., 2016. Temporal and phylogenetic evolution of the sauropod dinosaur body plan. R. Soc. Open Sci. 3, 150636.

Bejan, A., Marden, J.H., 2006. Unifying constructal theory for scale effects in running, swimming and flying. J. Exp. Biol. 209, 238–248.

Biewener, A.A., 1989. Mammalian terrestrial locomotion and size. Bioscience 39, 776–783.

Birn-Jeffery, A.V., Hubicki, C.M., Blum, Y., Renjewski, D., Hurst, J.W., Daley, M.A., 2014. Don't break a leg: running birds from quail to ostrich prioritise leg safety and economy on uneven terrain. J. Exp. Biol. 217, 3786–3796.

Blackburn, T.M., Gaston, K.J., Loder, N., 1999. Geographic gradients in body size: a clarification of Bergmann's rule. Divers. Distrib. 5, 165–174.

Bliese, P., 2006. Multilevel Modeling in R (2.2)–A Brief Introduction to R, the multilevel package and the nlme package. October.

Blomberg, S.P., Lefevre, J.G., Wells, J.A., Waterhouse, M., 2012. Independent contrasts and PGLS regression estimators are equivalent. Syst. Biol. 61, 382–391.

Bonnan, M. F., Shulman, J., Varadharajan, R., Gilbert, C., Wilkes, M., Horner, A., Brainerd, E., 2016. Forelimb kinematics of rats using XROMM, with implications for small eutherians and their fossil relatives. PloS one 11.

Bowker, R.M., Van Wulfen, K.K., Springer, S.E., Linder, K.E., 1998. Functional anatomy of the cartilage of the distal phalanx and digital cushion in the equine foot and a hemodynamic flow hypothesis of energy dissipation. Am. J. Vet. Res. 59, 961–968.

Brainerd, E.L., Baier, D.B., Gatesy, S.M., Hedrick, T.L., Metzger, K.A., Gilbert, S.L., Crisco, J.J., 2010. X-ray reconstruction of moving morphology (XROMM): precision, accuracy and applications in comparative biomechanics research. J. Exp. Zool. Part Ecol. Integr. Physiol. 313, 262–279.

Carrano, M. T., 1997. Morphological indicators of foot posture in mammals: a statistical and biomechanical analysis. Zool. J. Linnean Soc. 121, 77-104.

Castanera, D., Vila, B., Razzolini, N.L., Falkingham, P.L., Canudo, J.I., Manning, P.L., Galobart, À., 2013. Manus track preservation bias as a key factor for assessing trackmaker identity and quadrupedalism in basal ornithopods. PLoS One 8, e54177.

Cheung, J.T.M., Zhang, M., Leung, A.K.-L., Fan, Y.-B., 2005. Three-dimensional finite element analysis of the foot during standing—a material sensitivity study. J. Biomech. 38, 1045–1054.

Chi, K.J., Roth, V.L., 2010. Scaling and mechanics of carnivoran footpads reveal the principles of footpad design. J. R. Soc. Interface 7, 1145–1155.
Cholewo, T.J., Love, S., 1999. Gamut boundary determination using alpha-shapes, in: Color and Imaging Conference. Society for Imaging Science and Technology, pp. 200–204.
Clack, J.A., 1997. Devonian tetrapod trackways and trackmakers; a review of the fossils and footprints. Palaeogeogr. Palaeoclimatol. Palaeoecol. 130, 227–250.
Clarke, KA., 2017. Principles of thermal ecology. Oxford University Press.
Coombs Jr, W. P., 1978. Theoretical aspects of cursorial adaptations in dinosaurs. Quarterly Rev. Biol. 53, 393-418.
Dunning Jr, J.B., 1992. CRC handbook of avian body masses. CRC press.
Falkingham, P.L., 2014. Interpreting ecology and behaviour from the vertebrate fossil track record. J. Zool. 292, 222–228.
Falkingham, P.L., Bates, K.T., Mannion, P.D., 2012. Temporal and palaeoenvironmental distribution of manus-and pes-dominated sauropod trackways. J. Geol. Soc. 169, 365–370.
Falkingham, P.L., Bates, K.T., Margetts, L., Manning, P.L., 2011a. The 'Goldilocks' effect: preservation bias in vertebrate track assemblages. J. R. Soc. Interface 8, 1142–1154.
Falkingham, P.L., Bates, K.T., Margetts, L., Manning, P.L., 2011b. Simulating sauropod manus-only trackway formation using finite-element analysis. Biol. Lett. 7, 142–145.
Falkingham, P. L., 2014a. Interpreting Ecology and Behaviour from the Vertebrate Fossil Track Record. J. Zool. 292, 222-228.
Falkingham, P.L., Gatesy, S. M., 2014b. The birth of a dinosaur footprint: Subsurface 3D motion reconstruction and discrete element simulation reveal track ontogeny. PNAS 111, 18279-18284.
Farley, C.T., Glasheen, J., McMahon, T.A., 1993. Running springs: speed and animal size. J. Exp. Biol. 185, 71–86.
Farlow, J.O., 1992. Sauropod tracks and trackmakers: integrating the ichnological and skeletal records. Zubia 10.
Fedak, M.A., Heglund, N.C., Taylor, C.R., 1982. Energetics and mechanics of terrestrial locomotion. II. Kinetic energy changes of the limbs and body as a function of speed and body size in birds and mammals. J. Exp. Biol. 97, 23–40.
Felsenstein, J., 1985. Phylogenies and the comparative method. Am. Nat. 125, 1–15.
Ferraro, J.V., Binetti, K.M., 2014. American alligator proximal pedal phalanges resemble human finger bones: Diagnostic criteria for forensic investigators. Forensic Sci. Int. 240, 151–e1.
Full, R.J., Kubow, T., Schmitt, J., Holmes, P., Koditschek, D., 2002. Quantifying dynamic stability and maneuverability in legged locomotion. Integr. Comp. Biol. 42, 149–157.
Garland, T., 1983. The relation between maximal running speed and body mass in terrestrial mammals. J. Zool. 199, 157–170.
Gatesy, S. M., 1991. Hind limbs movements of the American alligator *(Alligator mississippiensis)* and postural grades. J. Zool. 224, 577-588.
Gatesy, S.M., Baier, D.B., Jenkins, F.A., Dial, K.P., 2010. Scientific rotoscoping: a morphology-based method of 3-D motion analysis and visualization. J. Exp. Zool. Part Ecol. Integr. Physiol. 313, 244–261.
Gatesy, S.M., Biewener, A.A., 1991. Bipedal locomotion: effects of speed, size and limb posture in birds and humans. J. Zool. 224, 127–147.

Gatesy, S. M., 2003. Direct and Indirect Track Features: What Sediment Did a Dinosaur Touch? Ichnos 10, 91-98.

Gatesy, S.M., Falkingham, P.L., 2017. Neither bones nor feet: track morphological variation and 'preservation quality.' J. Vertebr. Paleontol. e1314298.

Gatesy, S.M., Middleton, K. M., Jenkins Jr, F. A., Shubin, N. H., 1999. Three-dimensional preservation of foot movements in Triassic theropod dinosaurs. Nature 399, 141–144.

Gauthier, J., Kluge, A.G., Rowe, T., 1988. Amniote phylogeny and the importance of fossils. Cladistics 4, 105–209.

Geyer, H., Seyfarth, A., Blickhan, R., 2006. Compliant leg behaviour explains basic dynamics of walking and running. Proc. R. Soc. Lond. B Biol. Sci. 273, 2861–2867.

Grafen, A., 1989. The phylogenetic regression. Philos. Trans. R. Soc. Lond. B. Biol. Sci. 326, 119–157.

Harmon, L.J., Weir, J.T., Brock, C.D., Glor, R.E., Challenger, W., 2008. GEIGER: investigating evolutionary radiations. Bioinformatics 24, 129–131.

Hatala, K.G., Dingwall, H.L., Wunderlich, R.E., Richmond, B.G., 2013. The relationship between plantar pressure and footprint shape. J. Hum. Evol. 65, 21–28.

Hatala, K.G., Wunderlich, R.E., Dingwall, H.L., Richmond, B.G., 2016. Interpreting locomotor biomechanics from the morphology of human footprints. J. Hum. Evol. 90, 38–48.

Heckel, F., Schwier, M., Peitgen, H.-O., 2009. Object-oriented application development with MeVisLab and Python. GI Jahrestag. 154, 1338–51.

Henderson, D.M., 2006. Burly gaits: centers of mass, stability, and the trackways of sauropod dinosaurs. J. Vertebr. Paleontol. 26, 907–921.

Hildebrand, M., 1980. The adaptive significance of tetrapod gait selection. Am. Zool. 20, 255–267.

Hinterhofer, C. H., Stanek, C. H., Haider, H., 2000. The effect of flat horseshoes, raised heels and lowered heels on the biomechanics of the equine hoof assessed by finite element analysis (FEA). J. Vet. Med. 47, 73-82.

Hodgins, J.K., Raibert, M.N., 1991. Adjusting step length for rough terrain locomotion. IEEE Trans. Robot. Autom. 7, 289–298.

Hutchinson, J.R., Delmer, C., Miller, C.E., Hildebrandt, T., Pitsillides, A.A., Boyde, A., 2011. From flat foot to fat foot: structure, ontogeny, function, and evolution of elephant "sixth toes." Science 334, 1699–1703.

Hutson, J.D., Hutson, K.N., 2014. A repeated-measures analysis of the effects of soft tissues on wrist range of motion in the extant phylogenetic bracket of dinosaurs: implications for the functional origins of an automatic wrist folding mechanism in Crocodilia. The Anatomical Record 297, 1228-1249

Jackson, S.J., Whyte, M.A., Romano, M., 2009. Laboratory-controlled simulations of dinosaur footprints in sand: a key to understanding vertebrate track formation and preservation. Palaios 24, 222–238.

Jannel, A., Nair, J. P., Panagiotopoulou, O., Romilio, A., Salisbury, S. W., 2019. 'Keep Your Feet on the Ground': Simulated Range of Motion and Hind Foot Posture of the Middle Jurassic Sauropod *Rhoetosaurus brownei* and its Implications for Sauropod Biology. J. Morph.

Kambic, R. E., Roberts, T. J., Gatesy, S. M., 2015. Guineafowl with a twist: asymmetric limb control in steady bipedal locomotion. J. Exp. Biol. 218, 3836-3844.

Kilbourne, B.M., Carrier, D.R., 2016. Manipulated Changes in Limb Mass and Rotational Inertia in Trotting Dogs (*Canis lupus familiaris*) and Their Effect on Limb Kinematics. J. Exp. Zool. Part Ecol. Genet. Physiol. 325, 665–674.

Kilbourne, B.M., Hoffman, L.C., 2013. Scale effects between body size and limb design in quadrupedal mammals. PLoS One 8, e78392.

Knaust, D., Hauschke, N., 2004. Trace fossils versus pseudofossils in Lower Triassic playa deposits, Germany. Palaeogeogr. Palaeoclimatol. Palaeoecol. 215, 87–97.

Kubo, T., Sakamoto, M., Meade, A., Venditti, C., 2019. Transitions Between Foot Postures are Associated with Elevated Rates of Body Size Evolution in Mammals. PNAS. 116, 2618-2623.

Li, R., Lockley, M.G., Makovicky, P.J., Matsukawa, M., Norell, M.A., Harris, J.D., Liu, M., 2008. Behavioral and faunal implications of Early Cretaceous deinonychosaur trackways from China. Naturwissenschaften 95, 185–191.

Lockley, M.G., Farlow, J.O., Meyer, C.A., 1994. *Brontopodus* and *Parabrontopodus* ichnogen. nov. and the significance of wide-and narrow-gauge sauropod trackways. Gaia 10, 135–145.

Lockley, M.G., Xing, L., 2015. Flattened fossil footprints: implications for paleobiology. Palaeogeogr. Palaeoclimatol. Palaeoecol. 426, 85–94.

Maddison, W.P., Maddison, D., 2001. Mesquite: a modular system for evolutionary analysis.

McGuigan, M. R., Wilson, A. M., 2003. The effect of gait and digital flexor muscle activation on limb compliance in the forelimb of the horse *Equus caballus.* J. Exp. Biol. 206, 1325-1336.

McMahon, T.A., 1975. Using body size to understand the structural design of animals: quadrupedal locomotion. J. Appl. Physiol. 39, 619–627.

Michilsens, F., Aerts, P., Van Damme, R., D'Août, K., 2009. Scaling of plantar pressures in mammals. J. Zool. 279, 236–242.

Miller, C.E., Basu, C., Fritsch, G., Hildebrandt, T., Hutchinson, J.R., 2008. Ontogenetic scaling of foot musculoskeletal anatomy in elephants. J. R. Soc. Interface 5, 465–475.

Minter, N. J., Braddy, S. J., Davis, R. B., 2007. Between a Rock and a Hard Place: Arthropod Trackways and Ichnotaxonomy. Lethaia 40, 365-375.

Morse, S.A., Bennett, M.R., Liutkus-Pierce, C., Thackeray, F., McClymont, J., Savage, R., Crompton, R.H., 2013. Holocene footprints in Namibia: the influence of substrate on footprint variability. Am. J. Phys. Anthropol. 151, 265–279.

Nery, M.F., González, D.J., Hoffmann, F.G., Opazo, J.C., 2012. Resolution of the laurasiatherian phylogeny: evidence from genomic data. Mol. Phylogenet. Evol. 64, 685–689.

Padian, K., Olsen, P. E., 1984. The Fossil Trackway *Pteraichnus:* Not Pterosaurian but Crocodilian. J. Palaeontol. 58, 178-184.

Panagiotopoulou, O., Pataky, T.C., Day, M., Hensman, M.C., Hensman, S., Hutchinson, J.R., Clemente, C.J., 2016. Foot pressure distributions during walking in African elephants (*Loxodonta africana*). Open Sci. 3, 160203.

Panagiotopoulou, O., Pataky, T.C., Hill, Z., Hutchinson, J.R., 2012. Statistical parametric mapping of the regional distribution and ontogenetic scaling of foot pressures during walking in Asian elephants (*Elephas maximus*). J. Exp. Biol. 215, 1584–1593.

Panagiotopoulou, O., Rankin, J. W., Gatesy, S. M., Hutchinson, J. R., 2016. A preliminary case study of the effect of shoe-wearing on the biomechanics of a horse's foot. PeerJ 4, e2164.

Paradis, E., Claude, J., Strimmer, K., 2004. APE: analyses of phylogenetics and evolution in R language. Bioinformatics 20, 289–290.

Pataky, T.C., Caravaggi, P., Savage, R., Parker, D., Goulermas, J.Y., Sellers, W.I., Crompton, R.H., 2008. New insights into the plantar pressure correlates of walking speed using pedobarographic statistical parametric mapping (pSPM). J. Biomech. 41, 1987–1994.

Patla, A.E., 2003. Strategies for dynamic stability during adaptive human locomotion. IEEE Eng. Med. Biol. Mag. 22, 48–52.

Platt, B.F., Hasiotis, S.T., 2006. Newly discovered sauropod dinosaur tracks with skin and foot-pad impressions from the Upper Jurassic Morrison Formation, Bighorn Basin, Wyoming, USA. Palaios 21, 249–261.

Pollitt, C. C., 2004. Anatomy and physiology of the inner hoof wall. Clinical Techniques in Equine Practice 3, 1, 3-21

Prum, R.O., Berv, J.S., Dornburg, A., Field, D.J., Townsend, J.P., Lemmon, E.M., Lemmon, A.R., 2015. A comprehensive phylogeny of birds (Aves) using targeted next-generation DNA sequencing. Nature 526, 569–573.

Qian, Z., Ren, L., Ding, Y., Hutchinson, J.R., Ren, L., 2013. A dynamic finite element analysis of human foot complex in the sagittal plane during level walking. PloS One 8, e79424.

Reilly, S. M., Elias, J. A., 1998. Locomotion in *Alligator mississippiensis*: kinematic effects of speed and posture and their relevance to the sprawling-to-erect paradigm. J. Exp. Biol 201, 2559-2574.

Regnault, S., Hermes, R., Hildebrandt, T., Hutchinson, J., Weller, R., 2013. Osteopathology in the feet of rhinoceroses: lesion type and distribution. J. Zoo Wildl. Med. 44, 918–927.

Revell, L.J., 2012. phytools: an R package for phylogenetic comparative biology (and other things). Methods Ecol. Evol. 3, 217–223.

Rosenbaum, D., Hautmann, S., Gold, M., Claes, L., 1994. Effects of walking speed on plantar pressure patterns and hindfoot angular motion. Gait Posture 2, 191–197.

Saitta, E. T., Rogers, C. , Brooker, R. A., Abbott, G. D., Kumar, S. , O'Reilly, S. S., Donohoe, P. , Dutta, S. , Summons, R. E., Vinther, J., 2017. Low fossilization potential of keratin protein revealed by experimental taphonomy. Palaeontology, 60: 547-556.

Schaller, N. U., D'Août, K., Villa, R., Herkner, B., Aerts, P., 2011. Toe function and dynamic pressure distribution in ostrich locomotion. J. Exp. Biol. 214, 1123-1130.

Schmitt, D., Hanna, J.B., 2004. Substrate alters forelimb to hindlimb peak force ratios in primates. J. Hum. Evol. 46, 237–252.

Seebacher, F., Elsworth, P. G., Franklin, C. F. Ontogenetic changes of swimming kinematics in a semi-aquatic reptile (*Crocodylus porosus*). Aus. J. Zool 51, 15-24.

Segal, A., Rohr, E., Orendurff, M., Shofer, J., O'Brien, M., Sangeorzan, B., 2004. The effect of walking speed on peak plantar pressure. Foot Ankle Int. 25, 926–933.

Snyder, R.C., 1962. Quadrupedal and bipedal locomotion of lizards. Copeia 1952, 64–70.

Taylor, C.R., Shkolnik, A., Dmi'el, R., Baharav, D., Borut, A., 1974. Running in cheetahs, gazelles, and goats: energy cost and limb configuration. Am. J. Physiol. Content 227, 848–850.

Van Sittert, S., Skinner, J., Mitchell, G., 2015. Scaling of the appendicular skeleton of the giraffe (*Giraffa camelopardalis*). J. Morphol. 276, 503–516.

Warner SE, Pickering P, Panagiotopoulou O, Pfau T, Ren L, Hutchinson JR., 2013. Size-Related Changes in Foot Impact Mechanics in Hoofed Mammals. PLoS ONE 8(1): e54784

Witmer, L.M., Thomason, J.J., 1995. The extant phylogenetic bracket and the importance of reconstructing soft tissues in fossils. Funct. Morphol. Vertebr. Paleontol. 1, 19–33.

Tables

Table 1 – Regressions and Confidence Intervals for Main Analyses

Analysis	Linear Regression	Linear R^2	Log Regression	Log R^2	95% CI	P value
Pose 1 - All limbs	y = 0.51x + 146.71	$R^2 = 0.94$	$y = 0.59x^{0.99}$	$R^2 = 0.99$	1.922 ± 0.06186	<2.2E-16
Pose 1 - Forelimbs	y = 0.45x + 641.27	$R^2 = 0.92$	$y = 0.52x^{0.99}$	$R^2 = 0.99$	1.916 ± 7.887E-02	3.27E-15
Pose 1 - Hindlimbs	y = 0.59x - 292.02	$R^2 = 0.97$	$y = 0.64x^{0.98}$	$R^2 = 0.99$	1.9229 ± 0.0632	<2E-16
Pose 2a -All limbs	y = 0.20x + 1303.8	$R^2 = 0.82$	$y = 0.87x^{0.91}$	$R^2 = 0.99$	3.9266 ± 0.3584	1.93E-11
Pose 2a -Forelimbs	y = 0.21x + 1345.4	$R^2 = 0.85$	$y = 0.69x^{0.93}$	$R^2 = 0.97$	3.9614 ± 0.3954	8.68E-09
Pose 2a -Hindlimbs	y = 0.19x + 1177.4	$R^2 = 0.79$	$y = 1.06x^{0.89}$	$R^2 = 0.96$	4.1603 ±0.4157	2.08E-10
Pose 2b - All limbs	y = 0.48x + 436.75	$R^2 = 0.87$	$y = 0.58x^{0.98}$	$R^2 = 0.97$	1.856 ± 0.1199	5.98E-15
Pose 2b - Forelimbs	y = 0.52x + 410.47	$R^2 = 0.89$	$y = 0.47x^{0.10}$	$R^2 = 0.97$	1.7074 ± 0.1388	3.39E-10
Pose 2b - Hindlimbs	y = 0.44x + 535.85	$R^2 = 0.89$	$y = 0.71x^{0.96}$	$R^2 = 0.97$	2.029 ± 0.139	4.83E-14
Pose 2c - All limbs	y = 0.74x - 700.51	$R^2 = 0.93$	$y = 0.49x^{1.00}$	$R^2 = 0.97$	1.279 ± 6.225E-02	<2.2E-16
Pose 2c - Forelimbs	y = 0.79x - 1120.2	$R^2 = 0.95$	$y = 0.40x^{1.02}$	$R^2 = 0.97$	1.211 ± 6.473E-02	3.03E-13
Pose 2c - Hindlimbs	y = 0.69x - 228.13	$R^2 = 0.92$	$y = 0.57x^{0.99}$	$R^2 = 0.97$	1.333 ± 7.677E-02	8.04E-16

Table 2 – Regressions and Confidence Intervals for Analysis Subgroups

Analysis	Linear Regression	Linear R^2	Log Regression	Log R^2	95% CI	P value
Unguligrade	y = 0.36x - 593.56	$R^2 = 0.95$	$y = 0.27x^{1.01}$	$R^2 = 0.97$	2.6121 ± 0.2903	0.000844
Digitigrade	y = 0.19x + 1823.1	$R^2 = 0.83$	$y = 2.02x^{0.84}$	$R^2 = 0.97$	4.336 ± 0.537	2.02E-06
Plantigrade	y = 0.74x + 1128.3	$R^2 = 0.96$	$y = 0.35x^{1.06}$	$R^2 = 0.99$	1.29686 ± 0.08747	1.25E-07
Terrestrial	y = 0.45x + 491.99	$R^2 = 0.91$	$y = 0.68x^{0.96}$	$R^2 = 0.91$	1.9998 ± 0.1769	4.25E-08
Semi-aquatic	y = 0.77x + 408.03	$R^2 = 1.00$	$y = 0.42x^{1.02}$	$R^2 = 0.99$	1.30129 ± 0.02233	4.26E-09
Erect Posture	y = 0.48x + 588.49	$R^2 = 0.89$	$y = 0.94x^{0.93}$	$R^2 = 0.95$	1.8517 ± 0.1486	1.37E-10
Sprawling Posture	y = 0.51x - 19.70	$R^2 = 0.99$	$y = 0.50x^{0.99}$	$R^2 = 1.00$	1.96139 ± 0.06779	1.13E-07
Birds	y = 0.59x + 32.25	$R^2 = 1.00$	$y = 0.87x^{0.96}$	$R^2 = 0.99$	1.69386 ± 0.01636	1.59E-09
Mammals	y = 0.48x + 903.78	$R^2 = 0.87$	$y = 0.57x^{0.98}$	$R^2 = 0.91$	1.8353 ± 0.2018	9.87E-07

Figure Legends

Figure 1 - Projected area calculated from 3D models. A) *Hippopotamus* Left forelimb, soft tissue and bones reconstructed from CT data. B) The soft tissue was cropped at a point representative of the area that would contact the ground during life. The bones were cropped based on the same posterior extent (pose 1). C) The alpha shape (pink) and the convex hull (green) were used to determine underfoot area of the bones alone and D) the soft tissue. E) Bones were laid flat for a more repeatable approach (pose 2). Where semi-digitigrade animals were treated as digitigrade (pose 2a) only bones in pink were used, where semi-digitigrade animals were treated as intermediate between digitigrade and plantigrade (pose 2b), blue and pink bones were used, and where semi-digitigrade animals were treated as plantigrade, all bones including those in green were used. F) Alpha shapes for poses 2a-c, where pink is 2a, blue is 2b, and green is 2c. G-K) Distinctive foot morphologies in the data set. Scale bar = 10cm for all but G, where scale bar = 1cm.

Figure 2 – Bar graph showing projected skin surface area as a percentage of projected skeletal surface area across all specimens in A) Pose 1, with phylogeny for context, and B) Pose 2 (for elephant, rhino, and hippo, main bar represents Pose 2b and additional bars show poses 2a and 2c). Silhouettes from Phylopic. Mammalia data are in purple, Aves data in red, Crocodylia data in green, Lepidosauria data in blue, and Lissamphibia in yellow.

Figure 3 – Log_{10} plots for projected skin surface area against projected skeletal surface area in A) Pose 1, for all limbs, B) For Pose 1, for forelimbs, C) For Pose 1, for hindlimbs, Silhouettes from Phylopic. All numbers rounded to two significant figures. Mammalia data are in purple, Aves data in red, Crocodylia data in green, Lepidosauria data in blue, and Lissamphibia in yellow.

Figure 4 - Log_{10} plots for projected skin surface area against projected skeletal surface area for A) Pose 2a, all limbs, B) Pose 2b, all limbs, and C) For Pose 2c, all limbs. Silhouettes from Phylopic. All numbers rounded to two significant figures. Mammalia data are in purple, Aves data in red, Crocodylia data in green, Lepidosauria data in blue, and Lissamphibia in yellow.

Supplementary Figure Legends

Supplementary material 1: Supplementary tables – Additional data including p-values for all analysis, calculated soft-tissue and skeletal areas, approximate body masses for all animals, data for analyses with smallest and largest taxa removed, and demonstration of utility using *Plateosaurus engelhardti*.

Supplementary material 2: Supplementary graphs – Plots for projected skin surface area against projected skeletal surface area in Pose 1 and Pose 2, presented as sub-groups by phylogeny and ecology.

Supplementary material 3: Supplementary outlines – Top-down projections of models used in study, showing alpha shapes and convex hulls.

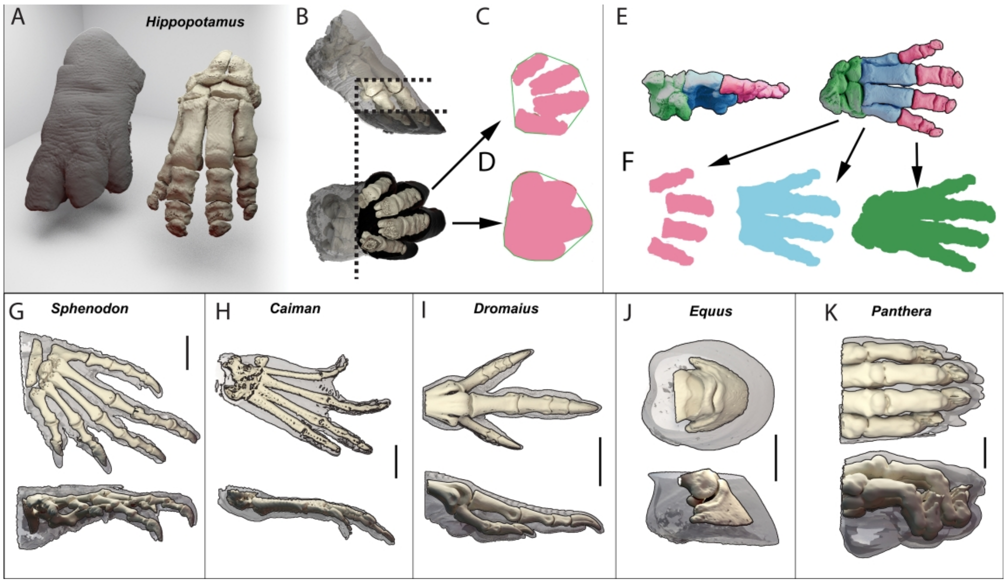

Figure 1 - Projected area calculated from 3D models. A) Hippopotamus Left forelimb, soft tissue and bones reconstructed from CT data. B) The soft tissue was cropped at a point representative of the area that would contact the ground during life. The bones were cropped based on the same posterior extent (pose 1). C) The alpha shape (pink) and the convex hull (green) were used to determine underfoot area of the bones alone and D) the soft tissue. E) Bones were laid flat for a more repeatable approach (pose 2). Where semi-digitigrade animals were treated as digitigrade (pose 2a) only bones in pink used, where semi-digitigrade animals were treated as intermediate between digitigrade and plantigrade (pose 2b), blue and pink bones were used, and where semi-digitigrade animals were treated as plantigrade, all bones including those in green were used. F) Alpha shapes for poses 2a-c, where pink is 2a, blue is 2b, and green is 2c. G-K) Distinctive foot morphologies in the data set. Scale bar = 10cm for all but G, where scale bar = 1cm.

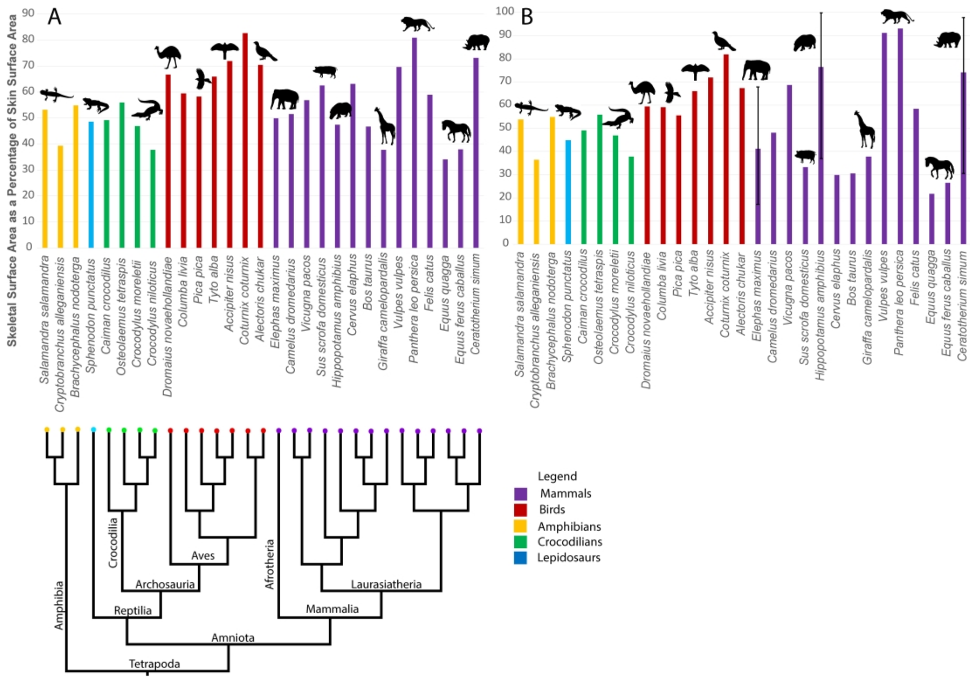

Figure 2 – Bar graph showing projected skin surface area as a percentage of projected skeletal surface area across all specimens in A) Pose 1, with phylogeny for context, and B) Pose 2 (for elephant, rhino, and hippo, main bar represents Pose 2b and additional bars show poses 2a and 2c). Silhouettes from Phylopic. Mammalia data are in purple, Aves data in red, Crocodylia data in green, Lepidosauria data in blue, and Lissamphibia in yellow.

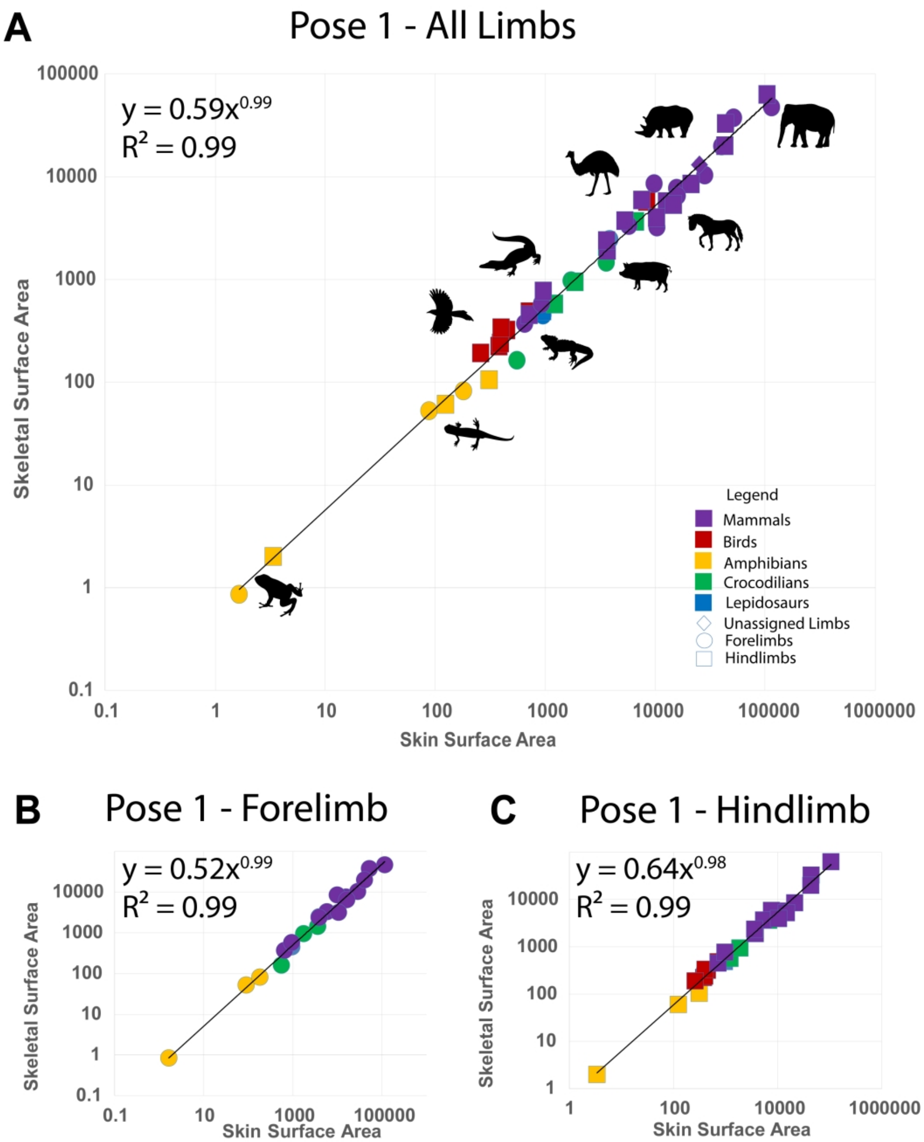

Figure 3 – Log10 plots for projected skin surface area against projected skeletal surface area in A) Pose 1, for all limbs, B) For Pose 1, for forelimbs, C) For Pose 1, for hindlimbs, Silhouettes from Phylopic. All numbers rounded to two significant figures. Mammalia data are in purple, Aves data in red, Crocodylia data in green, Lepidosauria data in blue, and Lissamphibia in yellow.

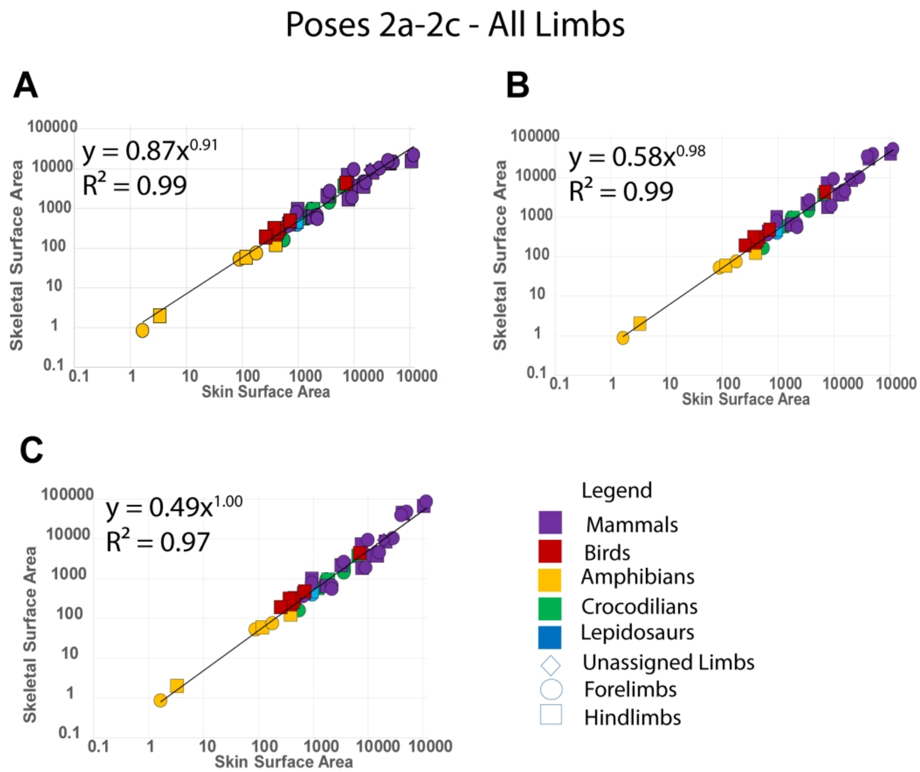

Figure 4 - Log10 plots for projected skin surface area against projected skeletal surface area for A) Pose 2a, all limbs, B) Pose 2b, all limbs, and C) For Pose 2c, all limbs. Silhouettes from Phylopic. All numbers rounded to two significant figures. Mammalia data are in purple, Aves data in red, Crocodylia data in green, Lepidosauria data in blue, and Lissamphibia in yellow.

Supplementary Tables

Supplementary Table 1 – Phylogenetic Comparative Tests for All Limbs in All Poses

		PIC			PGLS			
Analysis	Adjusted R²	CI	SE	P value	CI	SE	T value	P value
Pose 1	0.92	2.24	0.124	2.20E-16	2,24	0.124	18.0588	<0.0001
Pose 2a	0.5228	3.3875	0.6019	5.67E-06	2.713	0.263	10.12195	<0.0001
Pose 2b	0.6601	2.0175	0.2711	5.28E-08	1.7171	0.086	19.86243	<0.0001
Pose 2c	0.8483	1.45E+00	0.1156	8.79E-13	1.044	0.08	12.97394	0.00E+00

Pagel's Lambda

	Combined Data	Forelimb	Hindlimb
Pose 1	1.027319	1.045933	1.030825
All Limbs	Pose 2a	Pose 2b	Pose 2c
	1.017103	1.030825	-0.87799

Supplementary Table 2 – Area (mm2) Measurements for All Animals and Proportions of Skeleton to Skin Surface Area (%)

Pose 1

Specimen	**Fore/Hind Foot**	**Skin SA**	**Skel SA**	**Skeleton as % of Skin**
Salamandra salamandra	Forefoot	88.93501	52.14457	58.6322122
Salamandra salamandra	Hindfoot	124.8898	59.64688	47.75962093
Cryptobranchus alleganiensis	Forefoot	181.4453	82.04254	45.21613433
Cryptobranchus alleganiensis	Hindfoot	311.3837	103.9794	33.39268462
Brachycephlus nodoterga	Forefoot	1.6515	0.852027	51.59112909
Brachycephlus nodoterga	Hindfoot	3.39012	1.973128	58.20229633
Sphenodon punctatus	Forefoot	962.9668	447.0096	46.42004335
Sphenodon punctatus	Hindfoot	960.4319	487.3412	50.74188493
Crocodylus niloticus	Forefoot	553.7884	162.1849	29.28643561
Crocodylus niloticus	Hindfoot	1228.612	566.4358	46.10373211
Osteolaemus teraspis	Forefoot	1733.117	962.1605	55.51618621
Osteolaemus teraspis	Hindfoot	3678.328	2070.685	56.29419196
Caiman crocodilus	Hindfoot	1902.971	935.316	49.15029816
Crocodylus moreletii	Forefoot	3619.647	1447.981	40.00337567
Crocodylus moreletii	Hindfoot	6721.266	3618.094	53.83053494
Alectoris chukar	Hindfoot	451.7428	318.1106	70.4185217
Tyto alba	Hindfoot	721.4122	475.5846	65.92411232
Pica pica	Hindfoot	382.6398	222.9701	58.2715291
Columba livia	Hindfoot	397.7637	236.5437	59.46839319
Coturnix coturnix	Hindfoot	404.1557	334.2137	82.69428892

Accipiter nisus	Hindfoot	262.7824	189.0737	71.95065971
Dromaius novaehollandiae	Hindfoot	8524.232	5689.942	66.75019735
Bos taurus	Forefoot	15663.52	7659.069	48.8974879
Bos taurus	Hindfoot	12739.92	5669.063	44.49841375
Elephas maximus	Forefoot	115297.7	47094.3	40.84583773
Elephas maximus	Hindfoot	106205	62562.12	58.90696806
Ceratotherium simum	Forefoot	52322.45	37586.9	71.8370514
Ceratotherium simum	Hindfoot	43938.84	32640.53	74.28627909
Vicugna pacos	Forefoot	3879.717	2447.911	63.09507459
Vicugna pacos	Hindfoot	3737.41	1889.661	50.56071099
Giraffa camelopardalis	Forefoot	28591.02	10324.47	36.11087691
Giraffa camelopardalis	Hindfoot	21393.04	8422.208	39.36892218
Panthera leo persica	Forefoot	9849.389	8485.304	86.15055843
Panthera leo persica	Hindfoot	7690.173	5819.748	75.6777249
Felis catus	Forefoot	651.6308	367.1313	56.34038863
Felis catus	Hindfoot	724.9928	446.6624	61.6092115
Equus ferus caballus	Forefoot	16103.96	6521.98	40.49922225
Equus ferus caballus	Hindfoot	14886.19	5258.705	35.32606867
Sus scrofa	Forefoot	5833.796	3301.937	56.60015442
Sus scrofa	Hindfoot	5410.751	3703.087	68.43944159
Cervus elaphus	Forefoot	3876.212	2398.473	61.87673137
Cervus elaphus	Hindfoot	3644.912	2343.958	64.30766863
Equus quagga	Forefoot	10510.49	3188.5	30.33636481
Equus quagga	Hindfoot	10438.59	3927.968	37.62927945
Camelus dromedarius	Unassigned	25222.78	12990.49	51.50299004
Vulpes vulpes	Forefoot	939.0155	575.1637	61.25178197
Vulpes vulpes	Hindfoot	974.4242	759.2161	77.91433447
Hippopotamus amphibius	Forefoot	40556.15	19879.08	49.01619162
Hippopotamus amphibius	Hindfoot	43485.7	19909.79	45.78468328
Pose 2				
Salamandra salamandra	Forefoot	88.93501	52.14457	58.6322122
Salamandra salamandra	Hindfoot	118.7929	58.1717	48.9690014
Cryptobranchus alleganiensis	Forefoot	179.4845	75.75179	42.2052092
Cryptobranchus alleganiensis	Hindfoot	398.9009	121.8758	30.55289108
Brachycephlus nodoterga	Forefoot	1.6515	0.852027	51.59112909
Brachycephlus nodoterga	Hindfoot	3.39012	1.973128	58.20229633
Sphenodon punctatus	Forefoot	962.9668	394.6228	40.97989334
Sphenodon punctatus	Hindfoot	960.432	467.5052	48.67655561
Crocodylus niloticus	Forefoot	553.7884	162.1849	29.28643561
Crocodylus niloticus	Hindfoot	1228.612	566.4358	46.10373211
Osteolaemus teraspis	Forefoot	1733.117	962.1605	55.51618621
Osteolaemus teraspis	Hindfoot	3678.328	2070.685	56.29419196
Caiman crocodilus	Hindfoot	1902.971	935.316	49.15029816
Crocodylus moreletii	Forefoot	3619.647	1447.981	40.00337567
Crocodylus moreletii	Hindfoot	6721.266	3618.094	53.83053494
Alectoris chukar	Hindfoot	463.5517	312.3395	67.37963874
Tyto alba	Hindfoot	721.4122	475.5846	65.92411232

Pica pica	Hindfoot	398.4393	221.1307	55.49920666
Columba livia	Hindfoot	430.617	254.0651	59.00024677
Coturnix coturnix	Hindfoot	374.0761	306.0736	81.82121905
Accipiter nisus	Hindfoot	262.7824	189.0737	71.95065971
Dromaius novaehollandiae	Hindfoot	7189.013	4273.903	59.45048029
Bos taurus	Forefoot	14860.38	4672.811	31.44475656
Bos taurus	Hindfoot	12400.11	3656.876	29.49067084
Elephas maximus	Forefoot pose 2a	115297.7	21888.71	18.98452046
Elephas maximus	Hindfoot pose 2a	106205	16361.32	15.40542458
Elephas maximus	Forefoot pose 2b	115297.7	53085.99	46.04255484
Elephas maximus	Hindfoot pose 2b	106205	39665.72	37.34827271
Elephas maximus	Forefoot pose 2c	115297.7	85872.49	74.47894594
Elephas maximus	Hindfoot pose 2c	106205	64990.32	61.19330515
Ceratotherium simum	Forefoot pose 2a	40263.47	15929.85	39.56403613
Ceratotherium simum	Hindfoot pose 2a	43571.67	14885.36	34.1629407
Ceratotherium simum	Forefoot pose 2b	50319.26	38994.05	77.49327689
Ceratotherium simum	Hindfoot pose 2b	43938.84	31147.23	70.88768228
Ceratotherium simum	Forefoot pose 2c	40263.47	40068.14	99.51486813
Ceratotherium simum	Hindfoot pose 2c	43571.67	43695.43	100.2840375
Vicugna pacos	Forefoot	3651.553	2680.183	73.39842765
Vicugna pacos	Hindfoot	3349.815	2141.799	63.93783478
Giraffa camelopardalis	Forefoot	28591.02	10324.47	36.11087691
Giraffa camelopardalis	Hindfoot	21393.04	8422.208	39.36892218
Panthera leo persica	Forefoot	9849.389	9416.026	95.60010391
Panthera leo persica	Hindfoot	7690.173	6969.753	90.63193541
Felis catus	Forefoot	651.6308	367.1313	56.34038863
Felis catus	Hindfoot	680.9717	412.0175	60.50435475
Equus ferus caballus	Forefoot	16103.96	4560.854	28.3213136
Equus ferus caballus	Hindfoot	14886.19	3679.188	24.71545112
Sus scrofa	Forefoot	2182.029	665.3783	30.49356342
Sus scrofa	Hindfoot	1730.437	621.656	35.92479041
Cervus elaphus	Forefoot	2213.147	556.7199	25.15511885
Cervus elaphus	Hindfoot	1835.489	631.2443	34.39107695
Equus quagga	Forefoot	9146.338	1911.856	20.902962
Equus quagga	Hindfoot	7881.42	1775.487	22.5275036
Camelus dromedarius	Unassigned	19383.7	9322.263	48.09331236
Vulpes vulpes	Forefoot	939.0155	789.1365	84.03871265
Vulpes vulpes	Hindfoot	974.4242	958.9808	98.41512652
Hippopotamus amphibius	Forefoot pose 2a	40263.47	15929.85	39.56403613
Hippopotamus amphibius	Hindfoot pose 2a	43571.67	14885.36	34.1629407
Hippopotamus amphibius	Forefoot pose 2b	40263.47	34742	86.28665173
Hippopotamus amphibius	Hindfoot pose 2b	43571.67	29026.14	66.61700047
Hippopotamus amphibius	Forefoot pose 2c	40263.47	40068.14	99.51486813
Hippopotamus amphibius	Hindfoot pose 2c	43571.67	43695.43	100.2840375

Supplementary Table 3 - Body Mass for Each Subject Animal, Source of Data, and F and p Values for GLS with Body Mass as a Predictor of Correlatory Power for All Poses

Species	**Body Mass (g)**	**Source**
Salamandra salamandra	19.1	Encyclopedia of Life
Cryptobranchus alleganiensis	358	Encyclopedia of Life
Brachycephalus nodoterga	1	Pires Jr et al, 2005 (Toxicon, vol. 45, issue 1, 73-79)
Sphenodon punctatus	700	Animal Diversity Web
Caiman crocodilus	2174	Hutchinson metadata (Crocbase)
Osteolaemus tetraspis	7820	Hutchinson metadata (Cocbase)
Crocodylus moreletii	14150	Hutchinson metadata (Crocbase)
Crocodylus niloticus	1336	Hutchinson metadata (Crocbase)
Dromaius novaehollandiae	34200	CRC Handbook of Avian Body Masses
Columba livia	358.7	Encyclopedia of Life
Pica pica	151.3865	Encyclopedia of Life
Tyto alba	520	Animal Diversity Web
Accipiter nisus	237.5	CRC Handbook of Avian Body Masses
Coturnix coturnix	112.5	Encyclopedia of Life
Alectoris chukar	503.5	CRC Handbook of Avian Body Masses
Elephas maximus	3269794.34	Pantheria
Camelus dromedarius	492714.47	Pantheria
Vicugna pacos	64900	Pantheria
Sus scrofa domesticus	84471.54	Pantheria
Hippopotamus amphibius	1536310.4	Pantheria
Cervus elaphus	240867.13	Pantheria
Bos taurus	618642.42	Pantheria
Giraffa camelopardalis	964654.73	Pantheria
Vulpes vulpes	4820.36	Pantheria
Panthera leo persica	158623.93	Pantheria
Felis catus	2884.8	Pantheria
Equus quagga	400000	Pantheria
Equus ferus caballus	403598.53	Pantheria
Ceratotherium simum	2285939.43	Pantheria

	Pose 1			Pose 2a	Pose 2b	Pose 2c
Body Mass GLS	Combined Data	Forelimb	Hindlimb	Combined Data	Combined Data	Combined Data
F-Statistic	0.6473	0.3169	1.0615	4.8346	0.0615	0.01384
p-value	0.4287	0.5813	0.8062	0.0374	0.8062	0.9073

Supplementary Table 4 – Slope Uncertainties for all Poses and Combinations of Limbs

	All Limbs 1	Forelimbs 1	Hindlimbs 1	All Limbs 2a	Forelimbs 2a	Hindlimbs 2a
Slope	1.83	2.05	1.66	3.82	3.74	4.08
Uncertainty (Slope)	0.07	0.14	0.05	0.28	0.42	0.42
Correlation Coefficient (R^2)	0.94	0.92	0.97	0.80	0.82	0.79
F Statistic	700.03	217.89	1006.50	182.37	80.86	95.99
Regression of Sum of Squares	2.62E+10	1.33E+10	1.27E+10	2.16E+10	1.13E+10	1.03E+10
Y-Intercept	551.14	-127.88	756.10	-2637.39	-2776.37	-2629.16
Uncertainty (Y-Intercept)	992.47	2047.32	742.55	1908.16	3271.67	2369.49
Standard Error for Y Estimate	6114.66	7825.46	3557.13	10892.56	11822.08	10379.59
Degrees of Freedom	47.00	18.00	26.00	47.00	18.00	26.00
Residual Sum of Squares	1.76E+09	1.10E+09	3.29E+08	5.58E+09	2.52E+09	2.80E+09

	All Limbs 2b	Forelimbs 2b	Hindlimbs 2b	All Limbs 2c	Forelimbs 2c	Hindlimbs 2c
Slope	1.83	1.71	2.03	1.27	1.23	1.32
Uncertainty (Slope)	0.10	0.14	0.14	0.05	0.07	0.08
Correlation Coefficient (R^2)	0.89	0.89	0.89	0.93	0.95	0.92
F Statistic	367.33	151.26	213.21	648.43	345.79	289.64
Regression of Sum of Squares	2.47E+10	1.29E+10	1.17E+10	2.54E+10	1.31E+10	1.21E+10
Y-Intercept	618.26	900.74	43.67	1652.98	1986.94	1142.07
Uncertainty (Y-Intercept)	1325.83	2363.94	1571.50	986.25	1534.95	1335.15
Standard Error for Y Estimate	8205.80	9233.32	7419.28	6255.62	6162.94	6452.82
Degrees of Freedom	47.00	18.00	26.00	47.00	18.00	26.00
Residual Sum of Squares	3.16E+09	1.53E+09	1.43E+09	1.84E+09	6.84E+08	1.08E+09

Supplementary Table 5 – List of Taxa Used with Common Names and Latin Names

Latin Name	Common Name
Salamandra salamandra	Salamandra
Cryptobranchus alleganiensis	Hellbender
Brachycephalus nodoterga	Saddleback Toad
Sphenodon punctatus	Tuatara
Caiman crocodilus	Nile Crocodile
Osteolaemus tetraspis	Dwarf Crocodile
Crocodylus moreletii	Spectacled Caiman
Crocodylus niloticus	Morelet's Crocodile
Dromaius novaehollandiae	Chukar
Columba livia	Barn Owl

Pica pica	Magpie
Tyto alba	Pigeon
Accipiter nisus	Quail
Coturnix coturnix	Sparrowhawk
Alectoris chukar	Emu
Elephas maximus	Cow
Camelus dromedarius	Elephant
Vicugna pacos	Rhinoceros
Sus scrofa domesticus	Alpaca
Hippopotamus amphibius	Giraffe
Cervus elaphus	Lion
Bos taurus	Cat
Giraffa camelopardalis	Horse
Vulpes vulpes	Pig
Panthera leo persica	Deer
Felis catus	Zebra
Equus quagga	Camel
Equus ferus caballus	Fox
Ceratotherium simum	Hippopotamus

Supplementary Table 6 – Examples of Results with Large and Small Animals Removed

	R Squared	Equation	Multiplier
Original Data	0.9877	y=0.5901x0.9865	1.671751
Without Largest	0.9848	y=0.6225x0.9777	1.569478
Without Smallest	0.9754	y=0.7582x0.9592	1.265102
Without Largest and Smallest	0.9636	y=0.969x0.9257	0.955315

Supplementary Table 7 – Example of Study Utility Using *Plateosaurus engelhardti*

Plateosaurus	Skeleton	Skin (Combined Estimate)	Skin (Manus and Pes Distinct)
Manus Area	0.0194	0.032398	0.0388
Pes Area	0.0605	0.101035	0.0968
Manus as % of Pes	32.0661157	32.0661157	40.08264

Plateosaurus		
	Body Mass (N)	7384
	CoM (%GAD)	20.43
	Manus Load	1508.5512
	Pes Load	5875.4488
Combined	Manus Pressure	46563.09649
	Pes Pressure	58152.6085
Separate	Manus Pressure	38880.18557

	Pes Pressure	60696.78512	

Skeleton	Area	Load	Pressure
Manus	0.0194	1508.5512	77760.37
Pes	0.0605	5875.4488	97114.86
Manus as % of Pes	32.0661157	25.67550584	80.07052

Combined (Skin)	Area	Load	Pressure
Manus	0.032398	1508.5512	46563.1
Pes	0.101035	5875.4488	58152.61
Manus as % of Pes	32.0661157	25.67550584	80.07052

Separate (Skin)	Area	Load	Pressure
Manus	0.0388	1508.5512	38880.19
Pes	0.0968	5875.4488	60696.79
Manus as % of Pes	40.08264463	25.67550584	64.05642

Supplementary References

Myers, P., Espinosa, R., Parr, C.S., Jones, T., Hammond, G.S. and Dewey, T.A., 2006. The animal diversity web. *Accessed October*, *12*(2006), p.2.

Dunning Jr, John B. *CRC Handbook of Avian Body Masses*. CRC press, 1992.

Hutchinson, J. R.. *Crocbase.* DOI 10.17605/OSF.IO/X38NH

Jones, Kate E., Jon Bielby, Marcel Cardillo, Susanne A. Fritz, Justin O'Dell, C. David L. Orme, Kamran Safi, Wes Sechrest, Elizabeth H. Boakes, and Chris Carbone. "PanTHERIA: A Species-Level Database of Life History, Ecology, and Geography of Extant and Recently Extinct Mammals." *Ecology* 90, no. 9 (2009): 2648–2648.

Pires Jr, Osmindo R., Antonio Sebben, Elisabeth F. Schwartz, Rodrigo AV Morales, Carlos Bloch Jr, and Carlos A. Schwartz. "Further Report of the Occurrence of Tetrodotoxin and New Analogues in the Anuran Family Brachycephalidae." *Toxicon* 45, no. 1 (2005): 73–79.

Wilson, Edward O. "The Encyclopedia of Life." *Trends in Ecology & Evolution* 18, no. 2 (2003): 77–80.

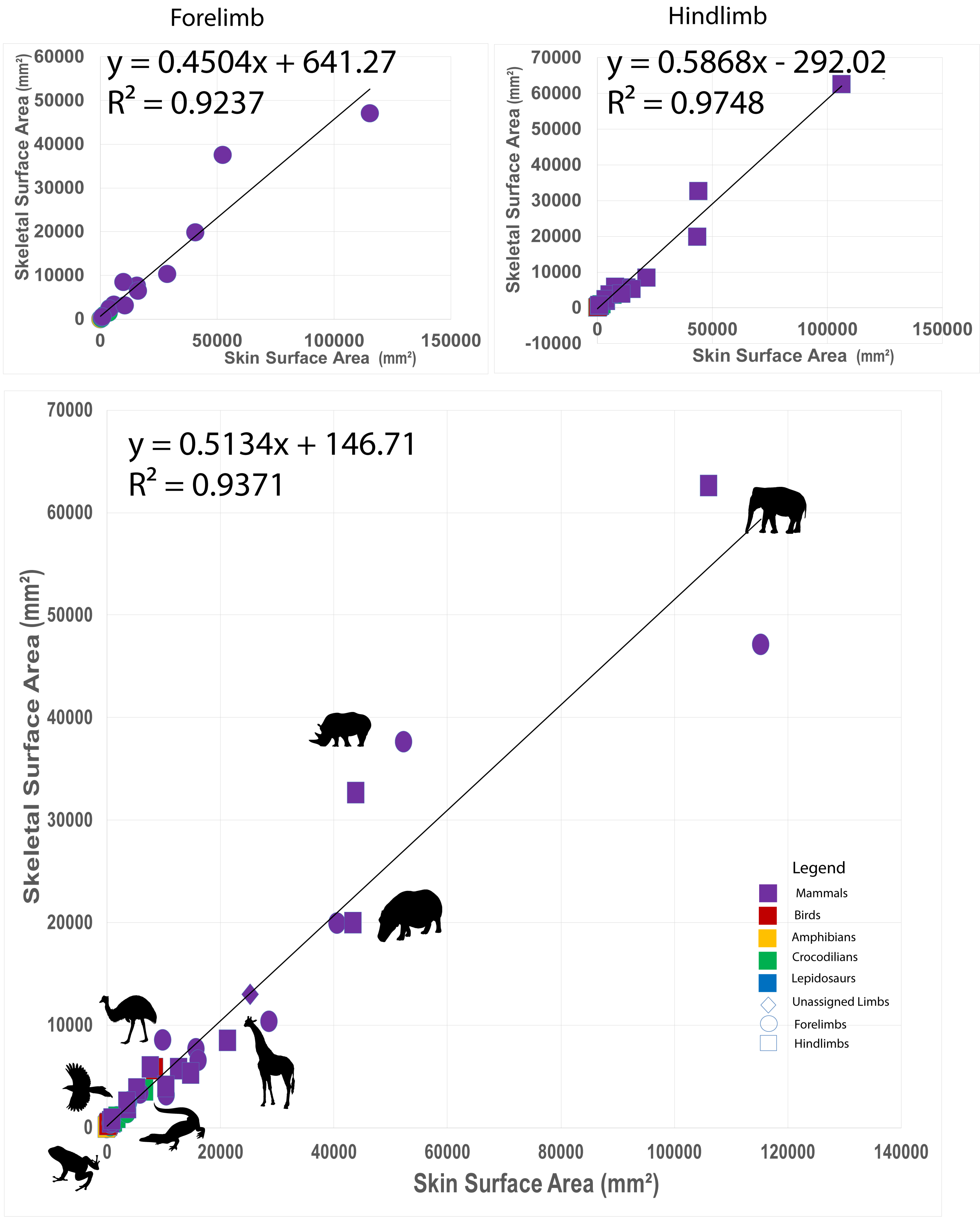

Linear plots for projected skin surface area against projected skeletal surface area in pose 1, for forelimbs, hindlimbs, and all limbs. Silhouettes from Phylopic.

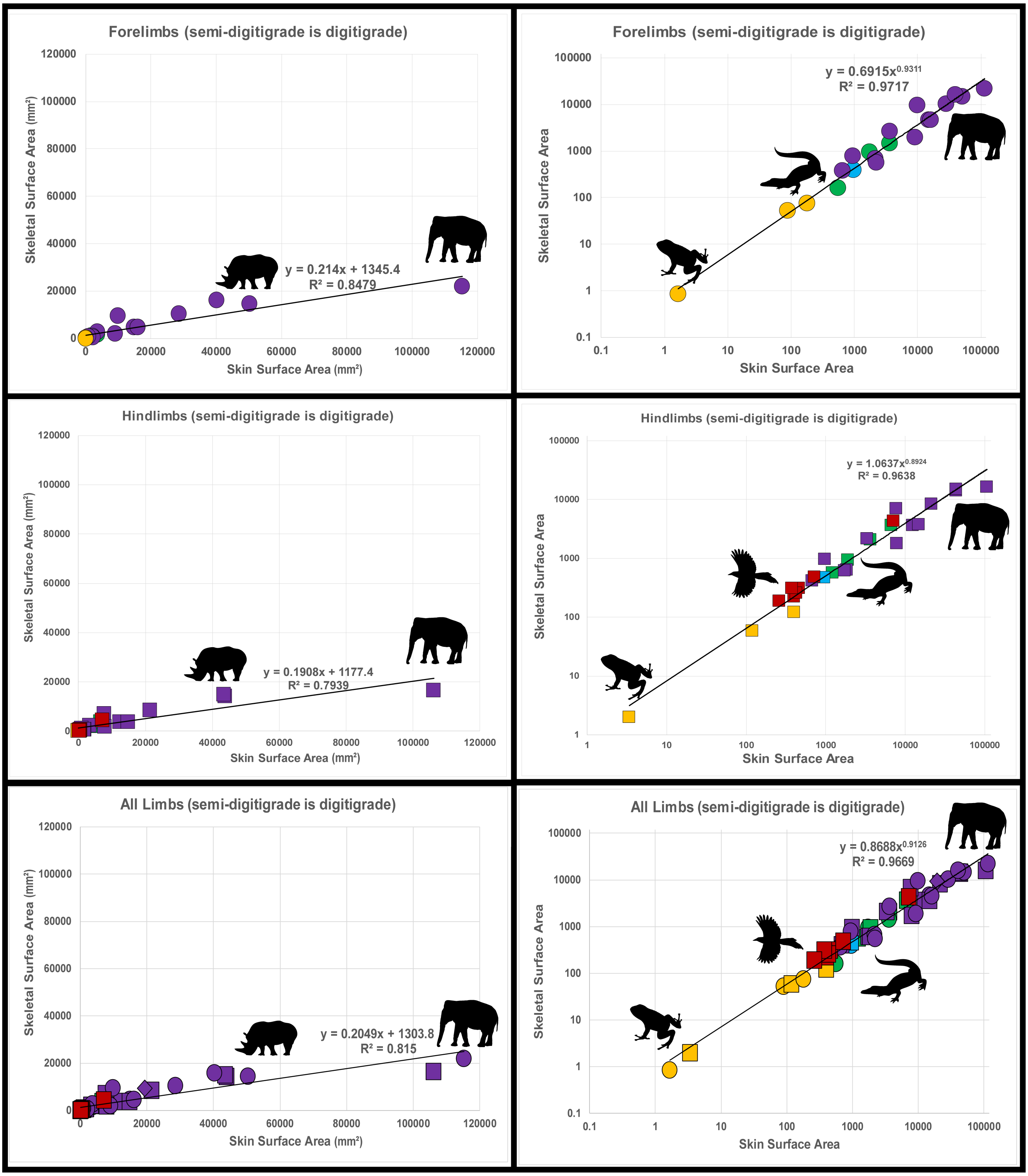

Linear and Log10-transformed plots for projected skin surface area against projected skeletal surface area, in pose 2a, for forelimbs, hindlimbs, and all limbs. Silhouettes from Phylopic.

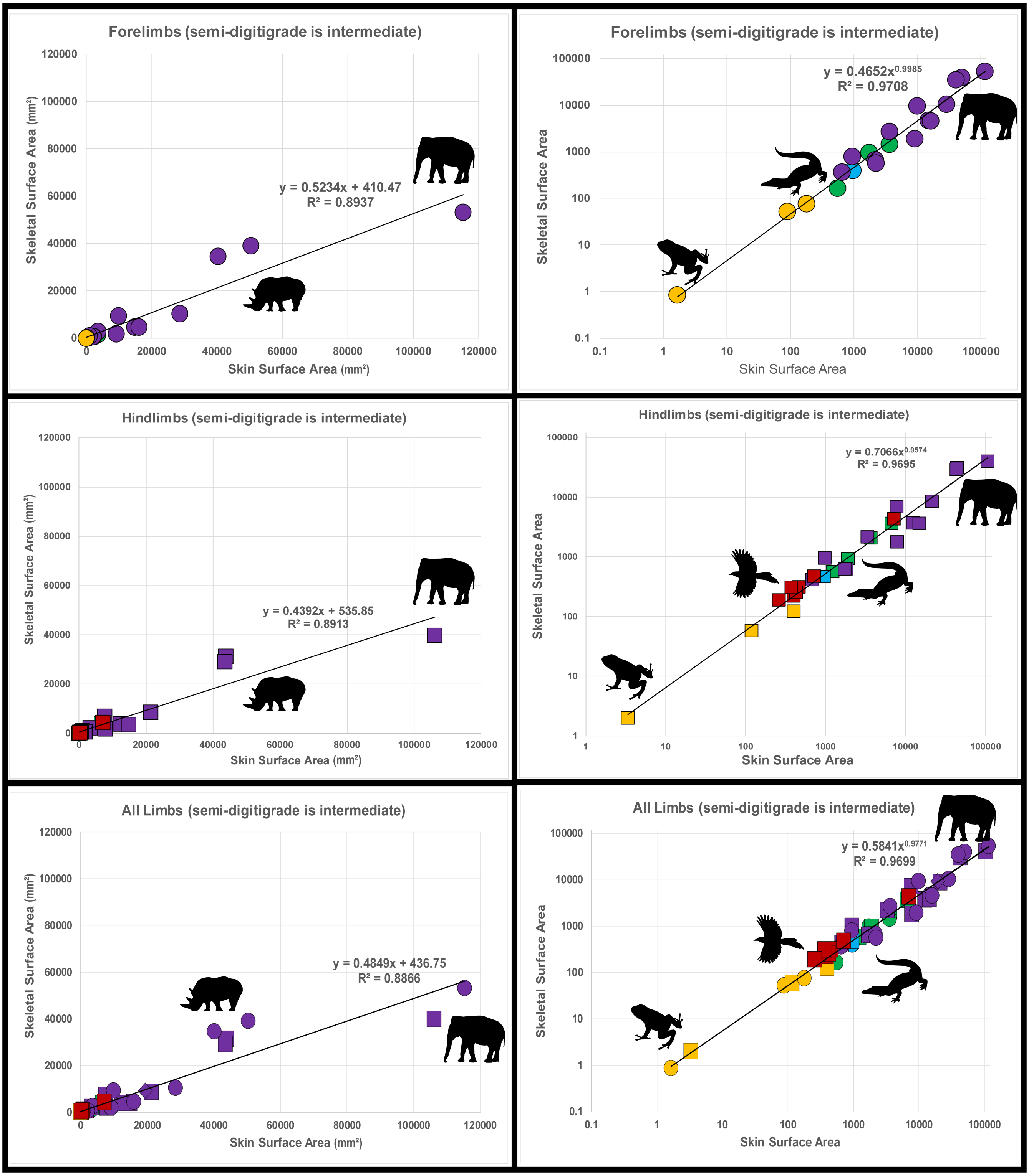

Linear and Log10-transformed plots for projected skin surface area against projected skeletal surface area, in pose 2b, for forelimbs, hindlimbs, and all limbs. Silhouettes from Phylopic.

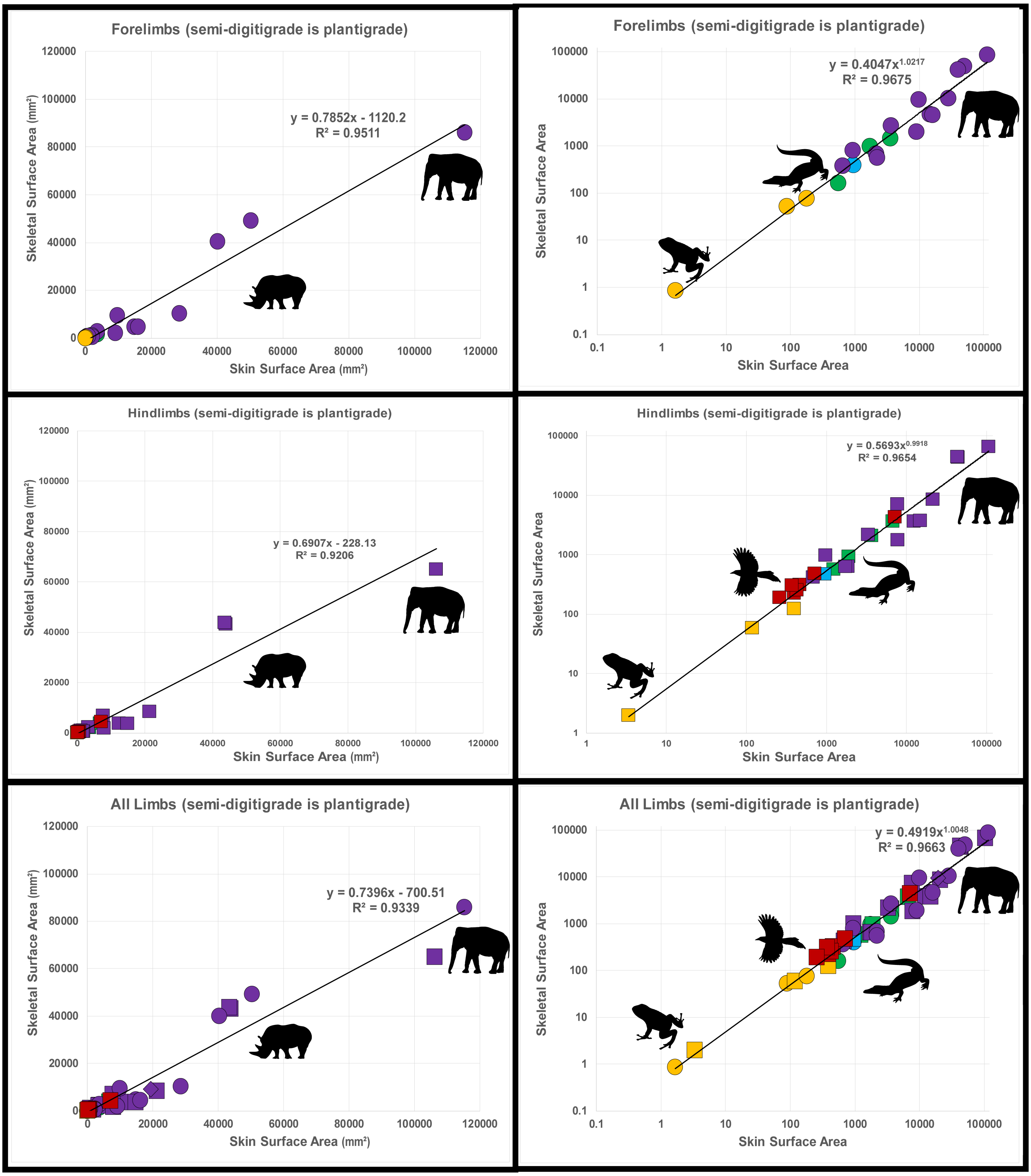

Linear and Log10-transformed plots for projected skin surface area against projected skeletal surface area, in pose 2c, for forelimbs, hindlimbs, and all limbs. Silhouettes from Phylopic.

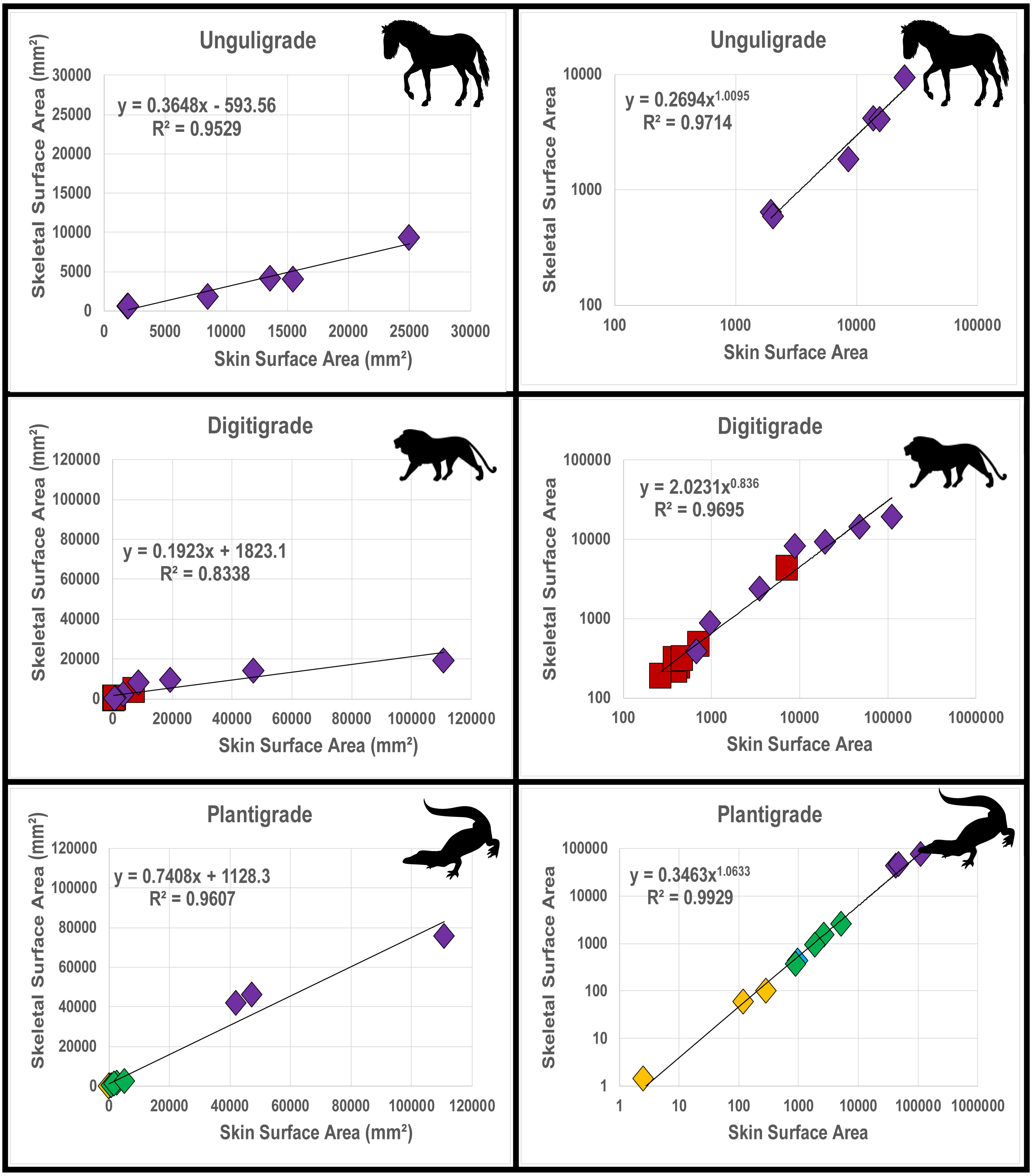

Linear and Log10-transformed plots for locomotor mode sub-analysis of projected skin surface area against projected skeletal surface area, in pose 2. Silhouettes from Phylopic.

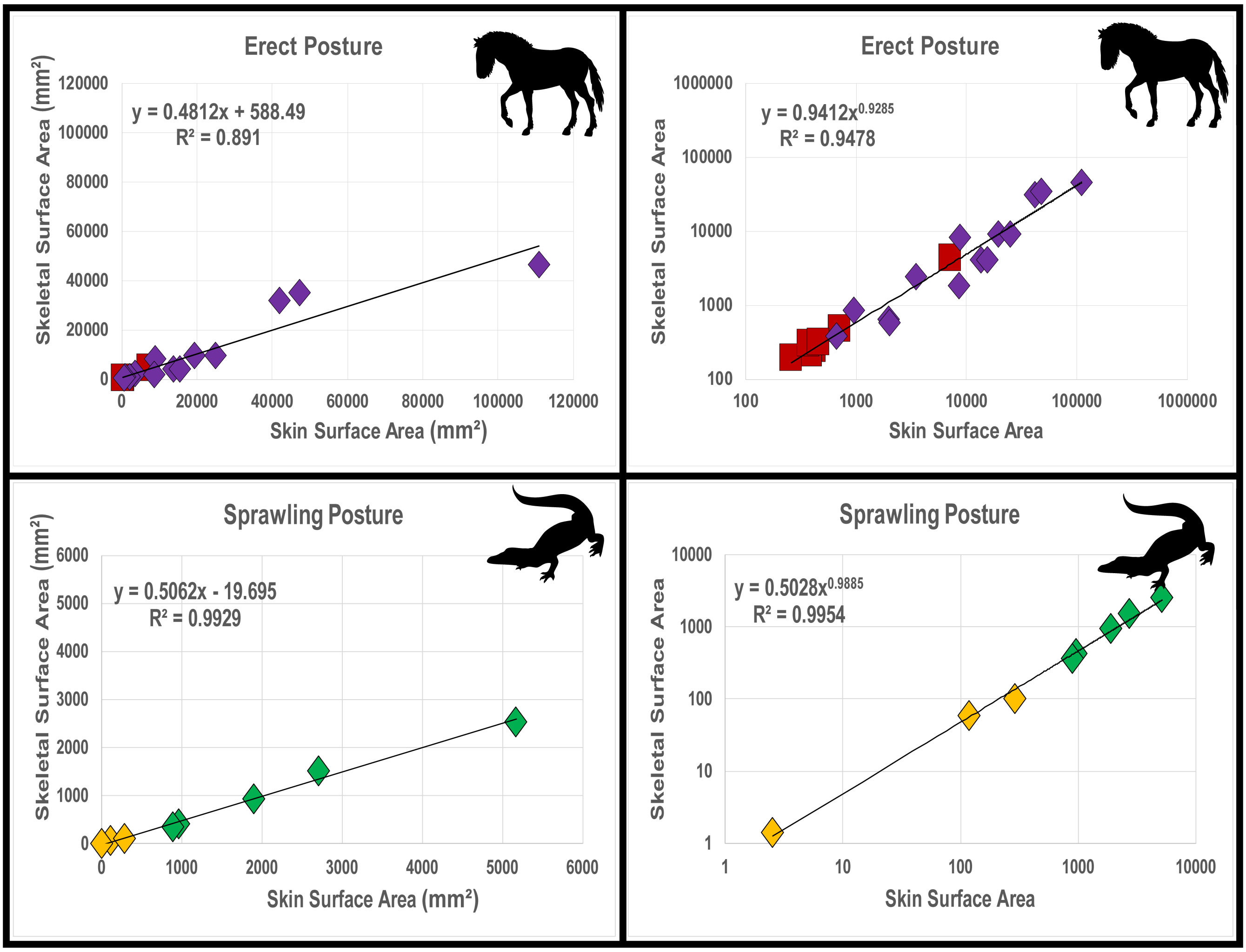

Linear and Log10-transformed plots for posture sub-analysis of projected skin surface area against projected skeletal surface area, in pose 2. Silhouettes from Phylopic.

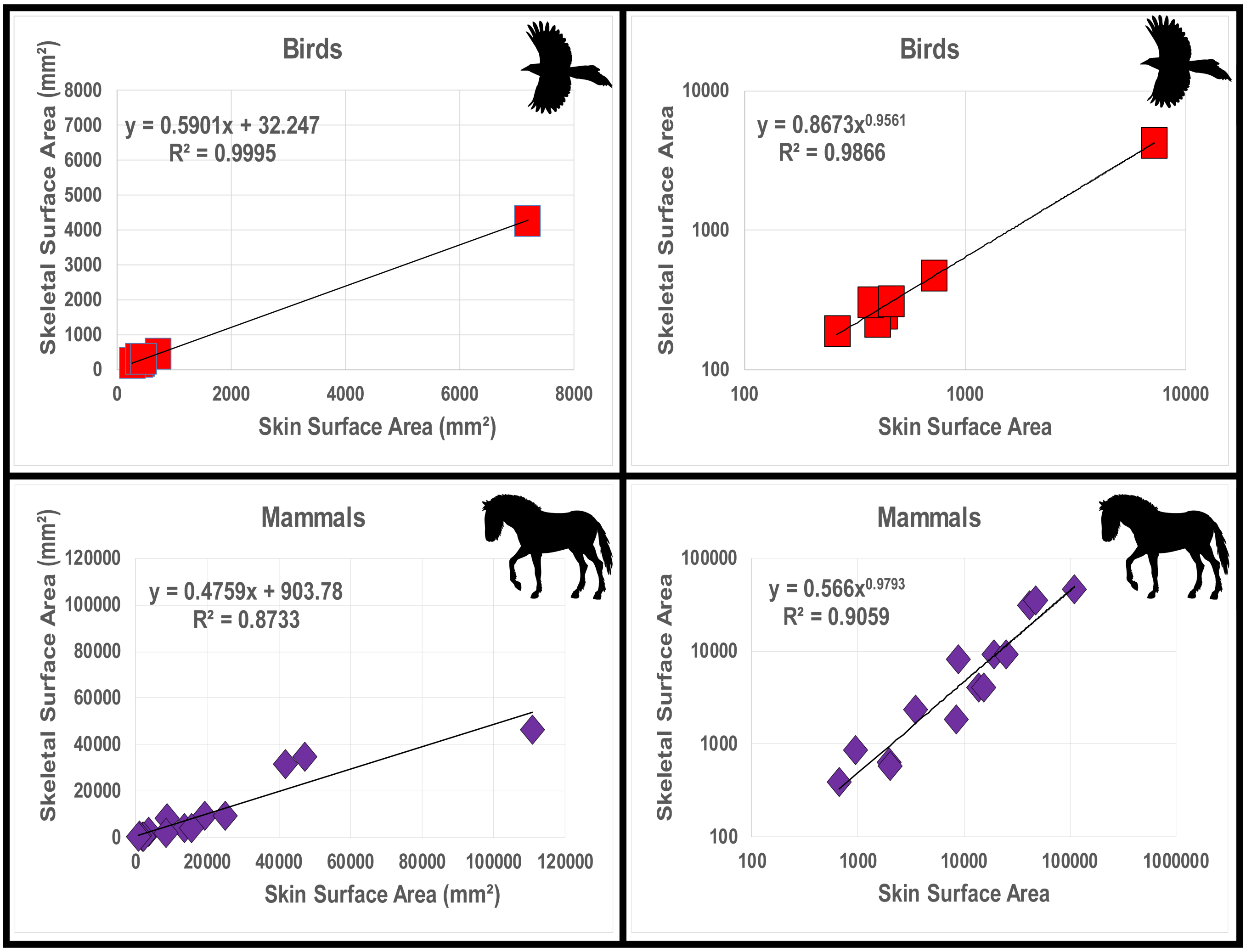

Linear and Log10-transformed plots for clade-based sub-analysis of projected skin surface area against projected skeletal surface area, in pose 2. Silhouettes from Phylopic.

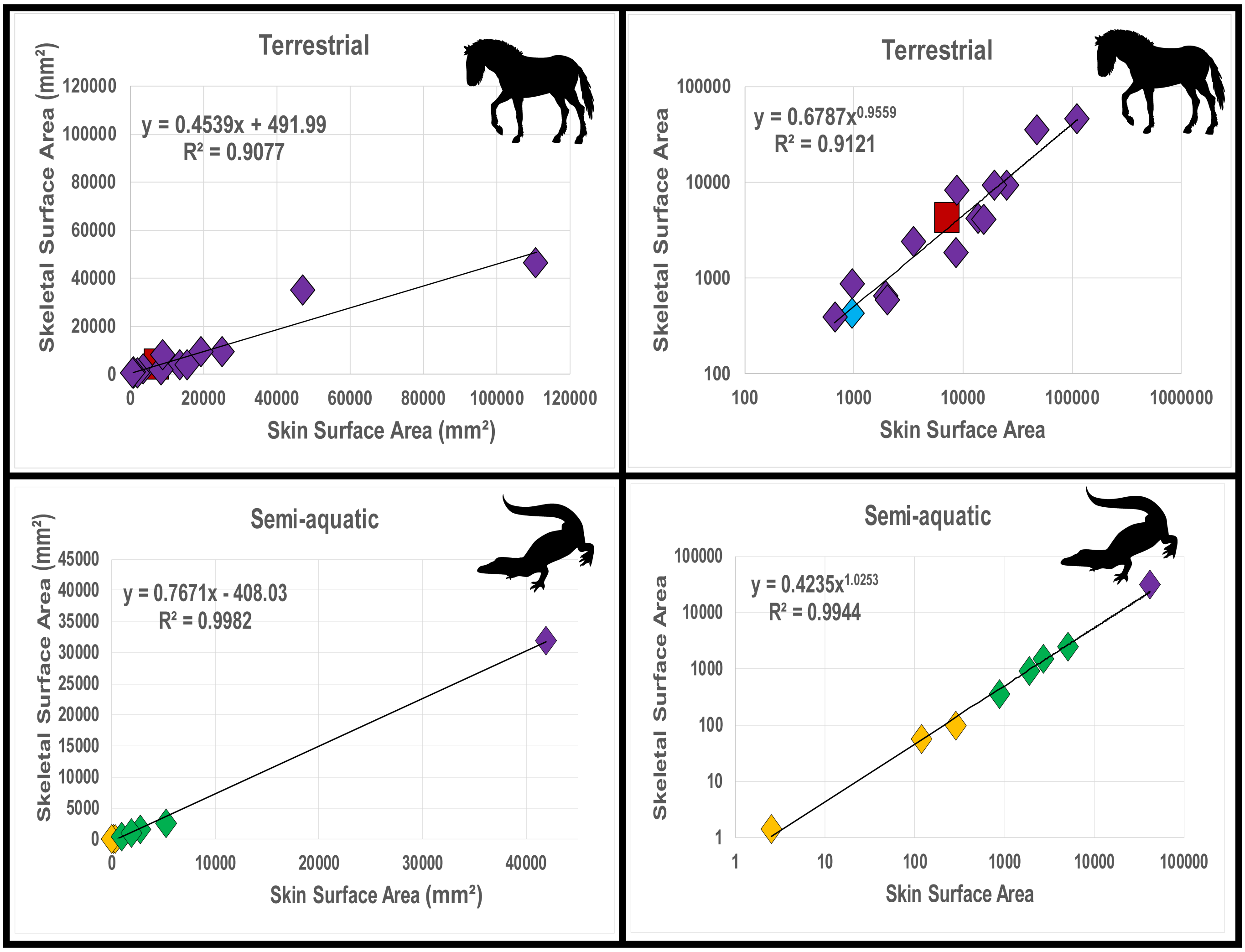

Linear and Log10-transformed plots for ecological sub-analysis of projected skin surface area against projected skeletal surface area, in pose 2. Silhouettes from Phylopic.

Supplemental Data

Presented here are the alpha shape outlines generated via matlab. Outlines are presented for skin surface area and skeletal area in pose 1 (approximate life position), and skeletal outlines for pose 2 (bones laid flat on the horizontal plane).

In some cases (e.g. many crocodilians), pose 1 and pose 2 were identical, as the foot bones are horizontal in both poses.

Large digitigrade/sub-unguligrade animals (Elephant, Hippo, and Rhino) which in life walk on a large fatty pad beneath the foot, had skeletal areas calculated in Pose 2 from just the digits (Pose 2a, as digitigrade), the digits and metatarsals/metacarpals (Pose2b, intermediate) and from the entire Pes/Manus (Pose 2c, as plantigrade).

All units are in mm, except the Tuatara where units are in 0.1mm.

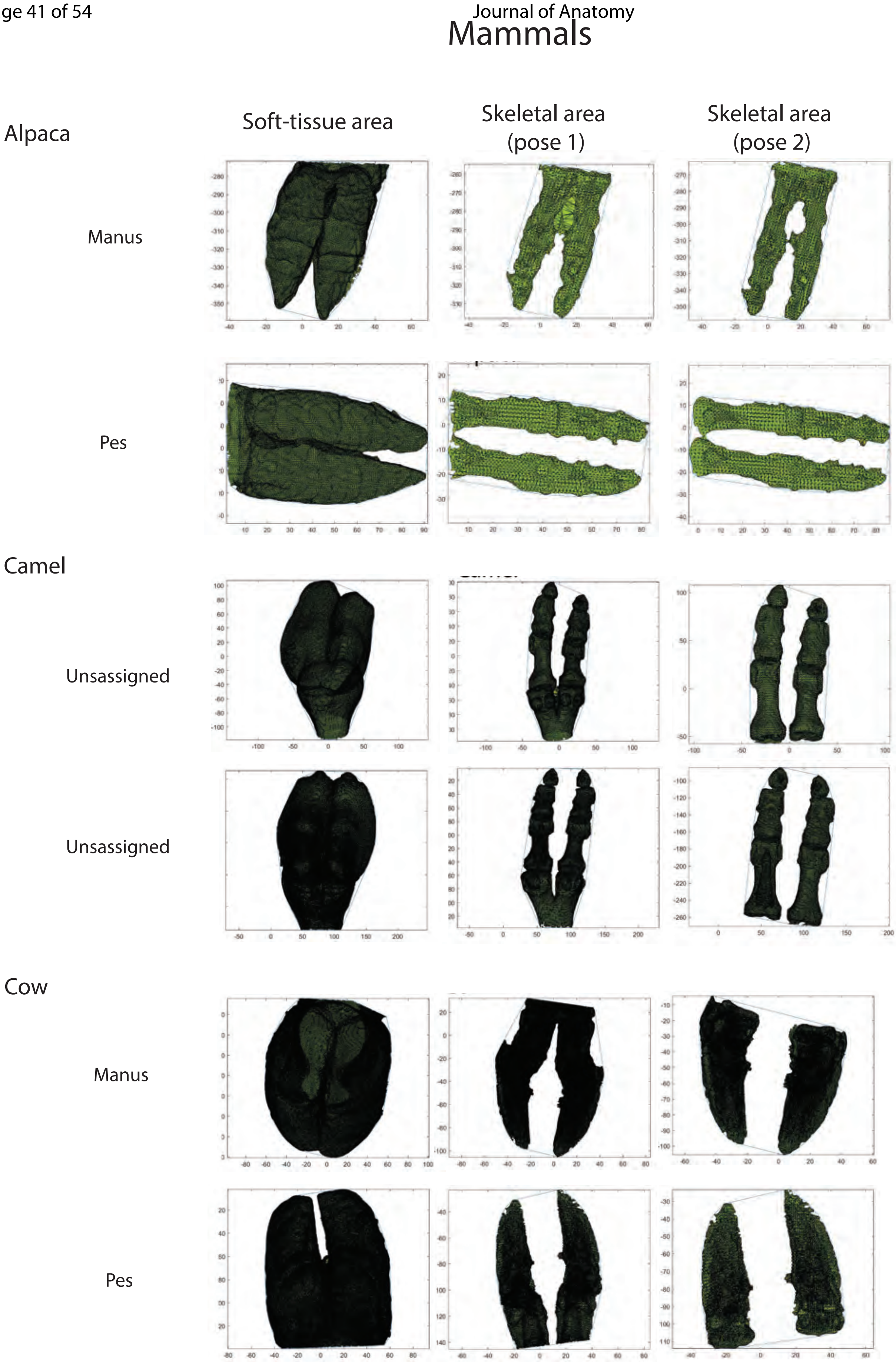
Mammals
Alpaca
Soft-tissue area
Skeletal area (pose 1)
Skeletal area (pose 2)
Manus
Pes
Camel
Unsassigned
Unsassigned
Cow
Manus
Pes

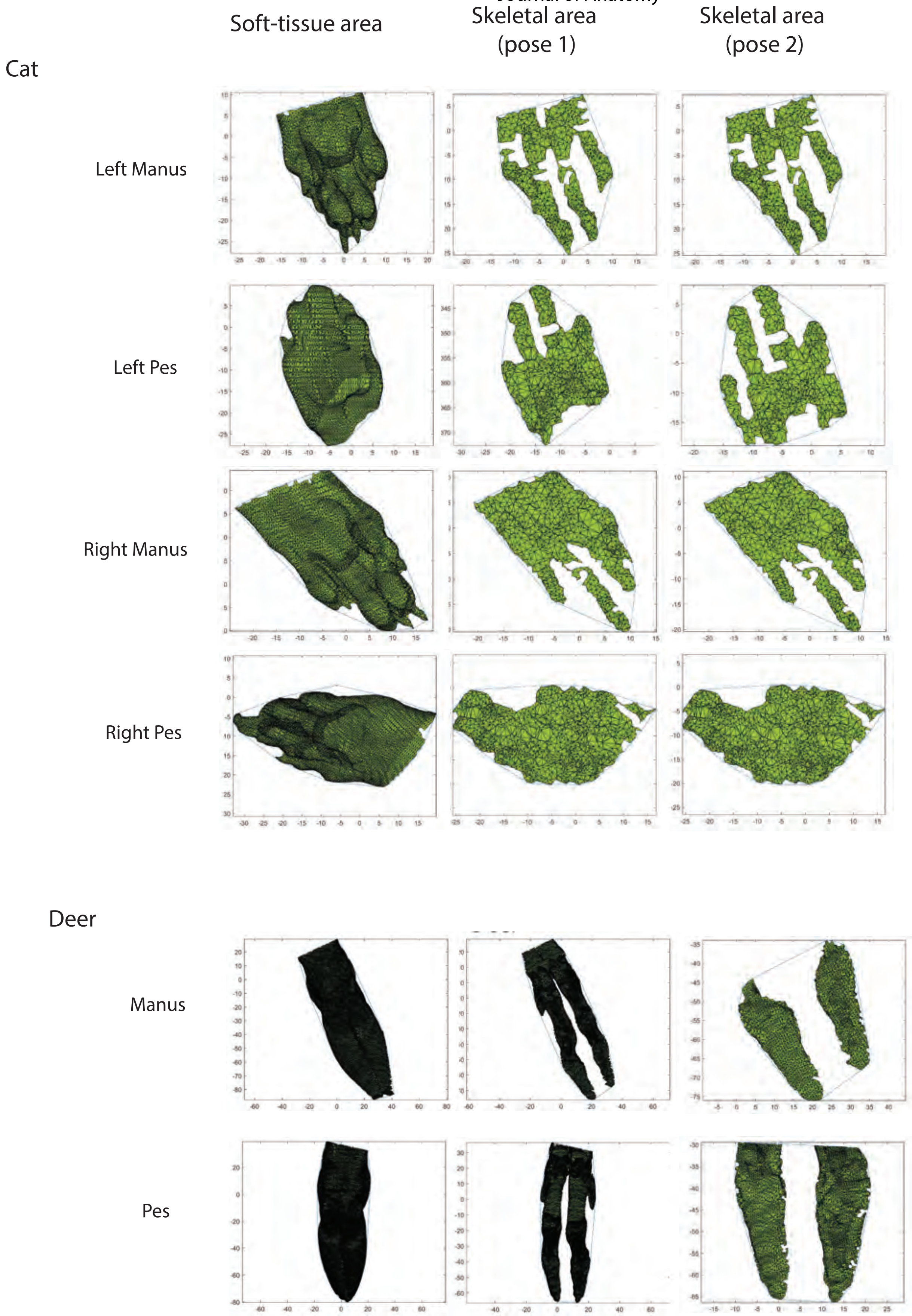
Soft-tissue area
Skeletal area (pose 1)
Skeletal area (pose 2)
Cat
Left Manus
Left Pes
Right Manus
Right Pes
Deer
Manus
Pes

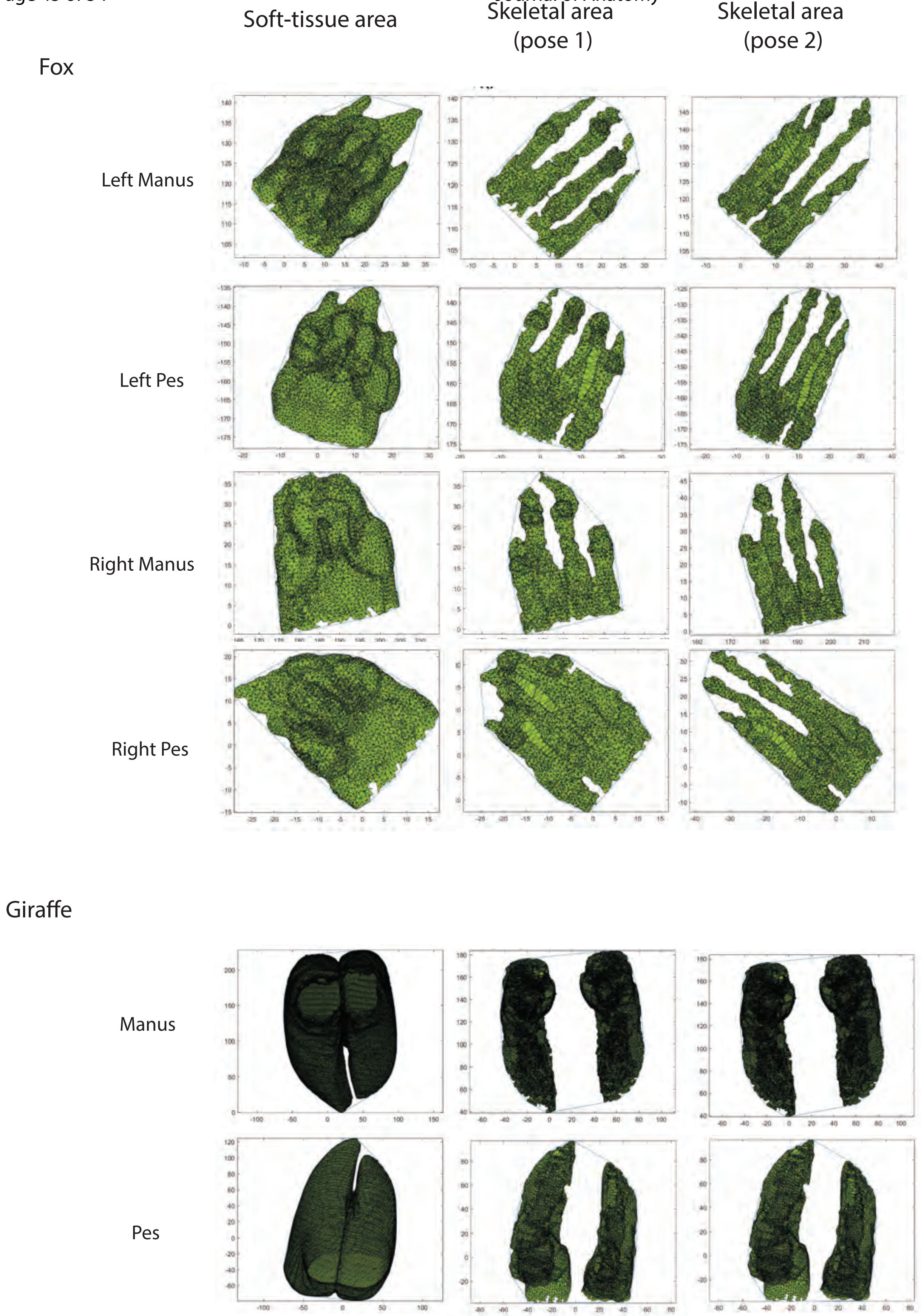
Soft-tissue area
Skeletal area (pose 1)
Skeletal area (pose 2)
Fox
Left Manus
Left Pes
Right Manus
Right Pes
Giraffe
Manus
Pes

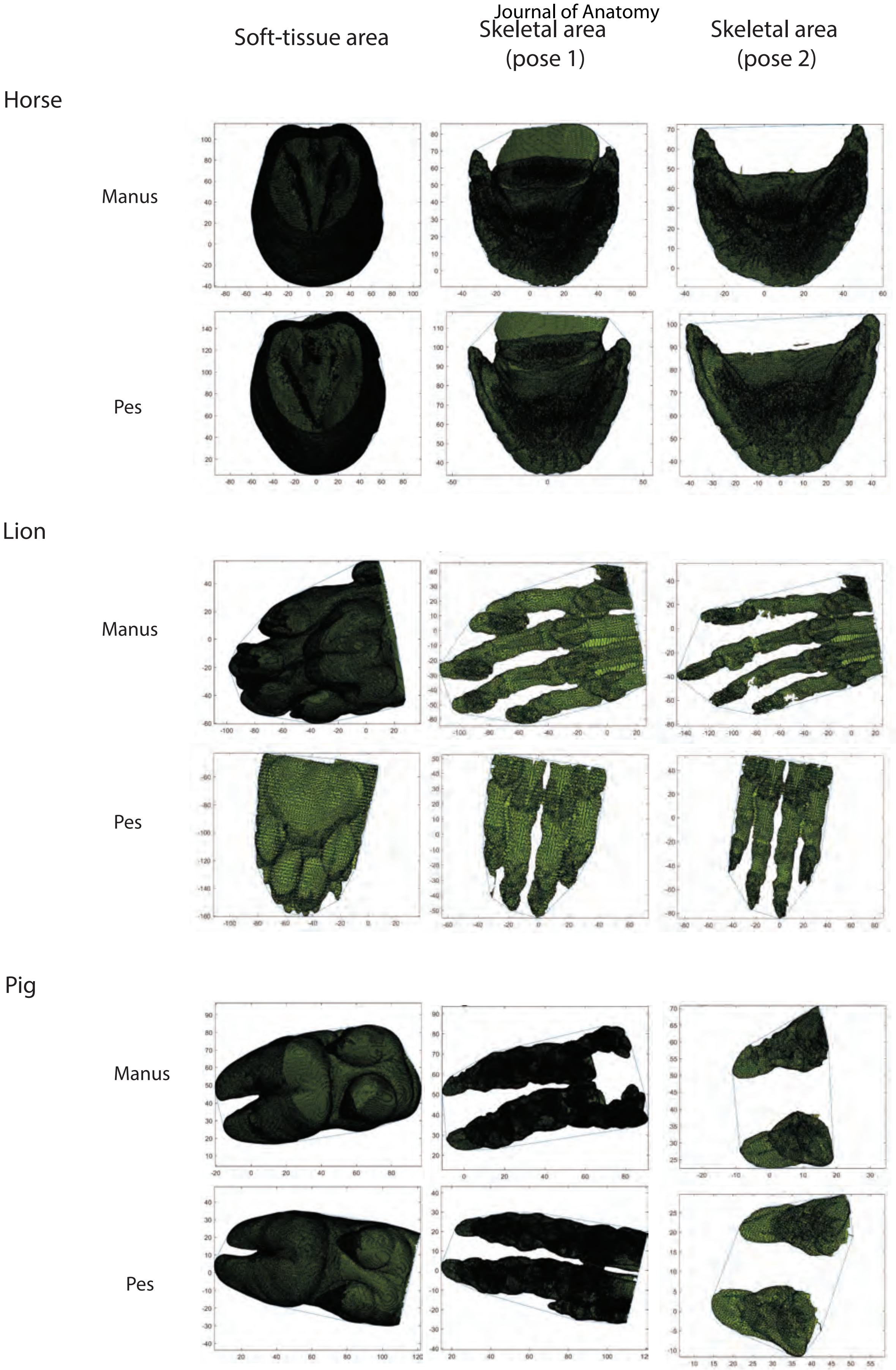
Soft-tissue area
Skeletal area (pose 1)
Skeletal area (pose 2)
Horse
Manus
Pes
Lion
Manus
Pes
Pig
Manus
Pes

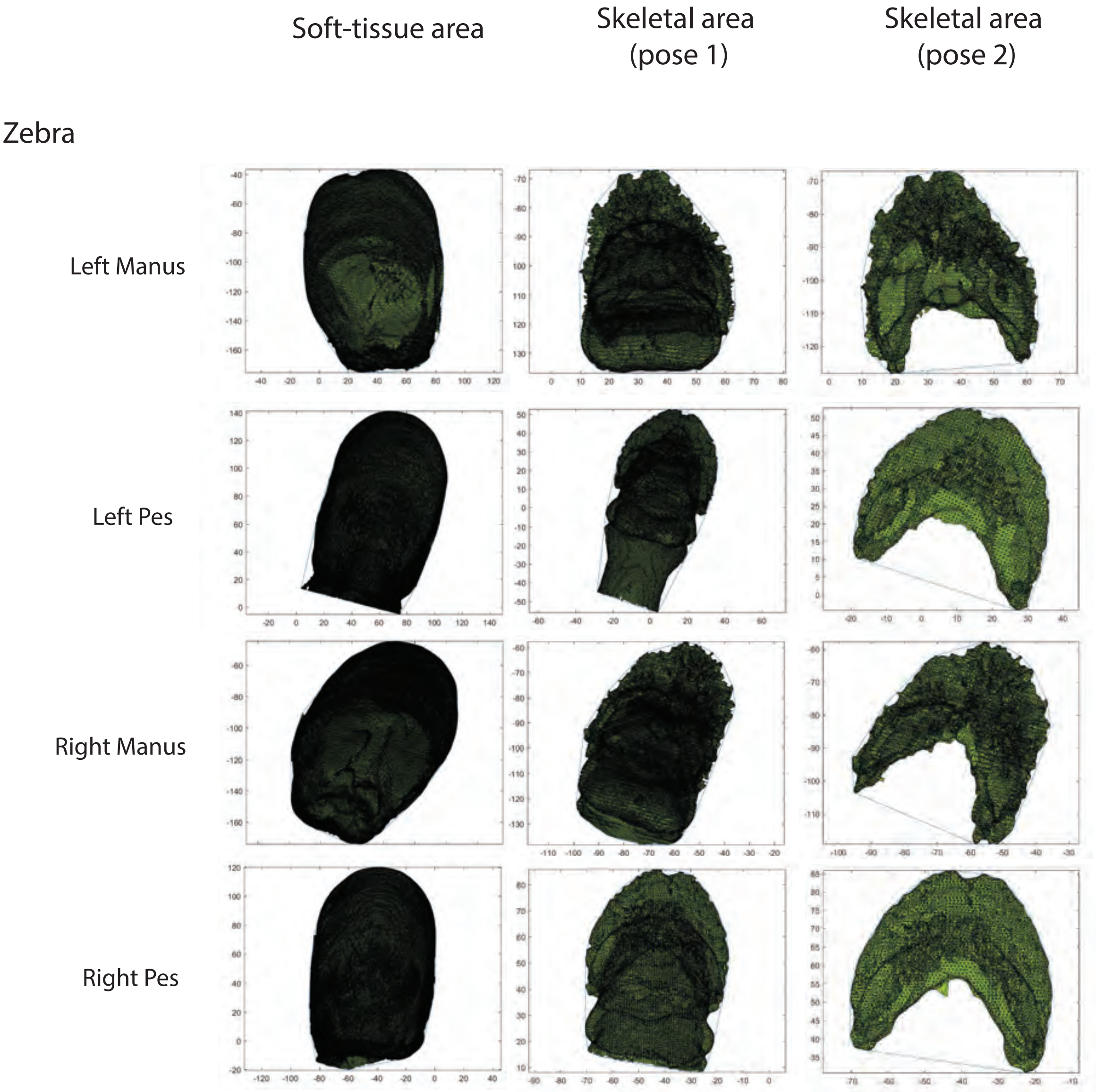

Soft-tissue area
Skeletal area (pose 1)
Skeletal area (pose 2)
Zebra
Left Manus
Left Pes
Right Manus
Right Pes

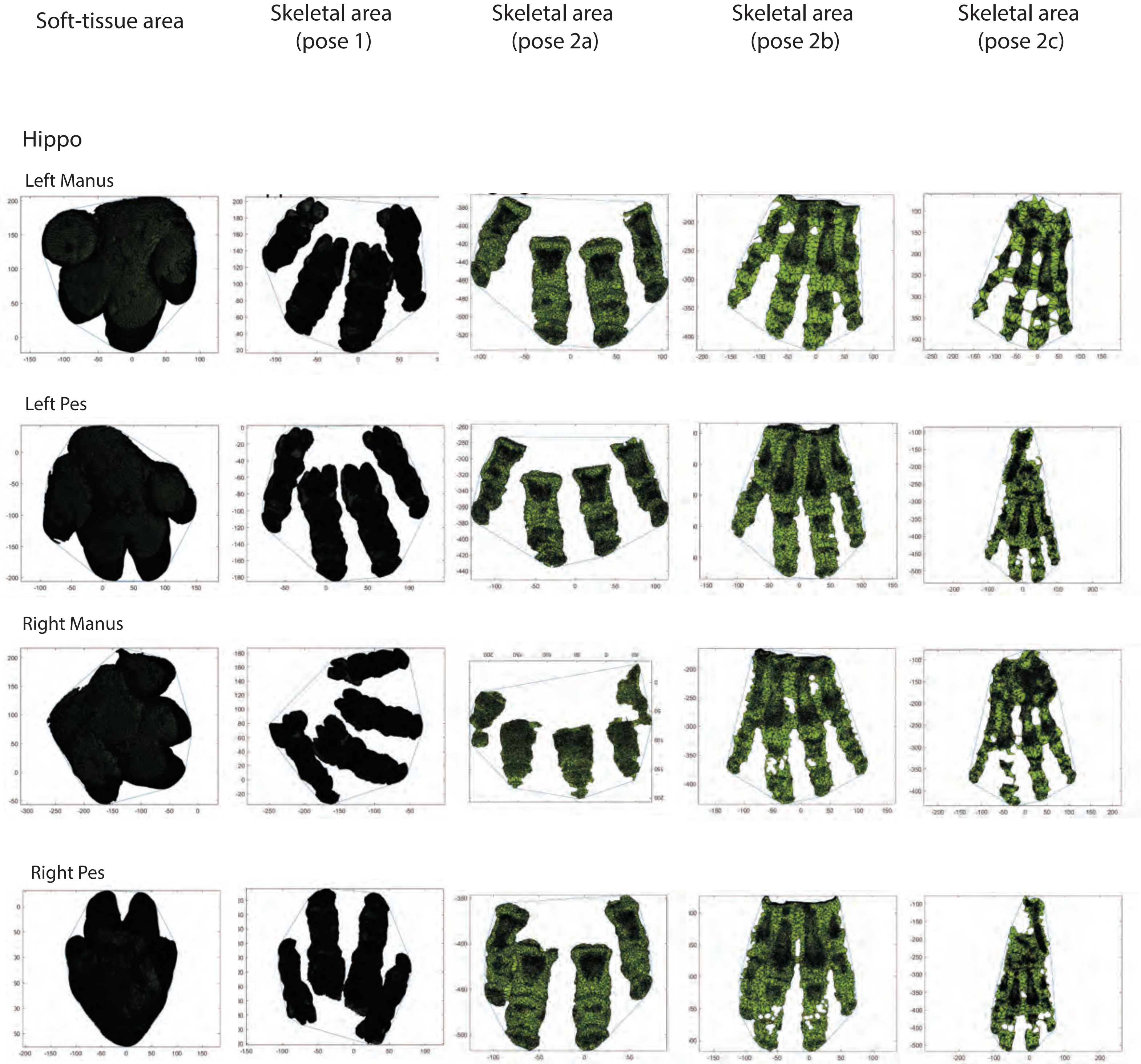
Soft-tissue area
Skeletal area (pose 1)
Skeletal area (pose 2a)
Skeletal area (pose 2b)
Skeletal area (pose 2c)
Hippo
Left Manus
Left Pes
Right Manus
Right Pes

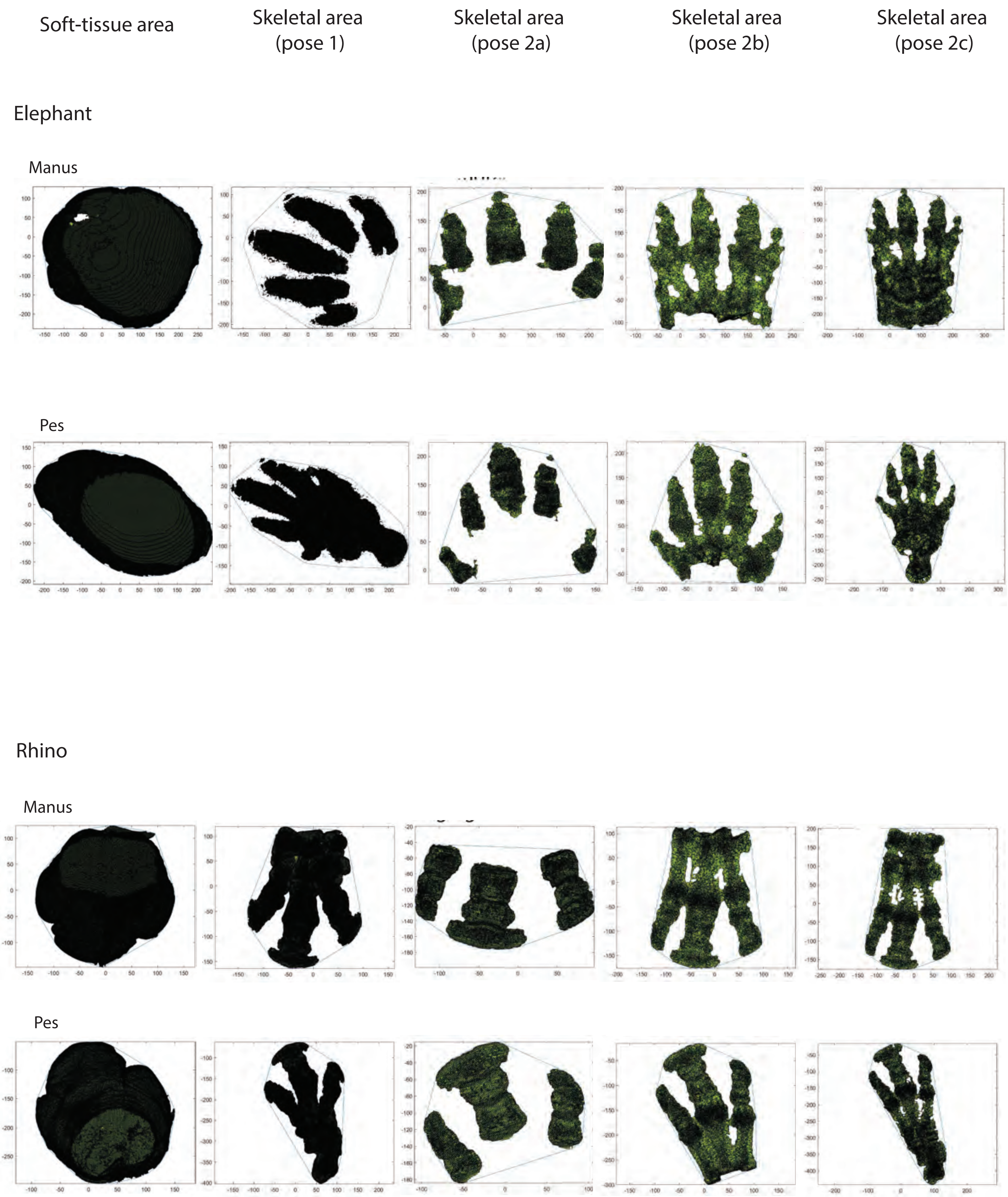

Soft-tissue area
Skeletal area (pose 1)
Skeletal area (pose 2a)
Skeletal area (pose 2b)
Skeletal area (pose 2c)
Elephant
Manus
Pes
Rhino
Manus
Pes

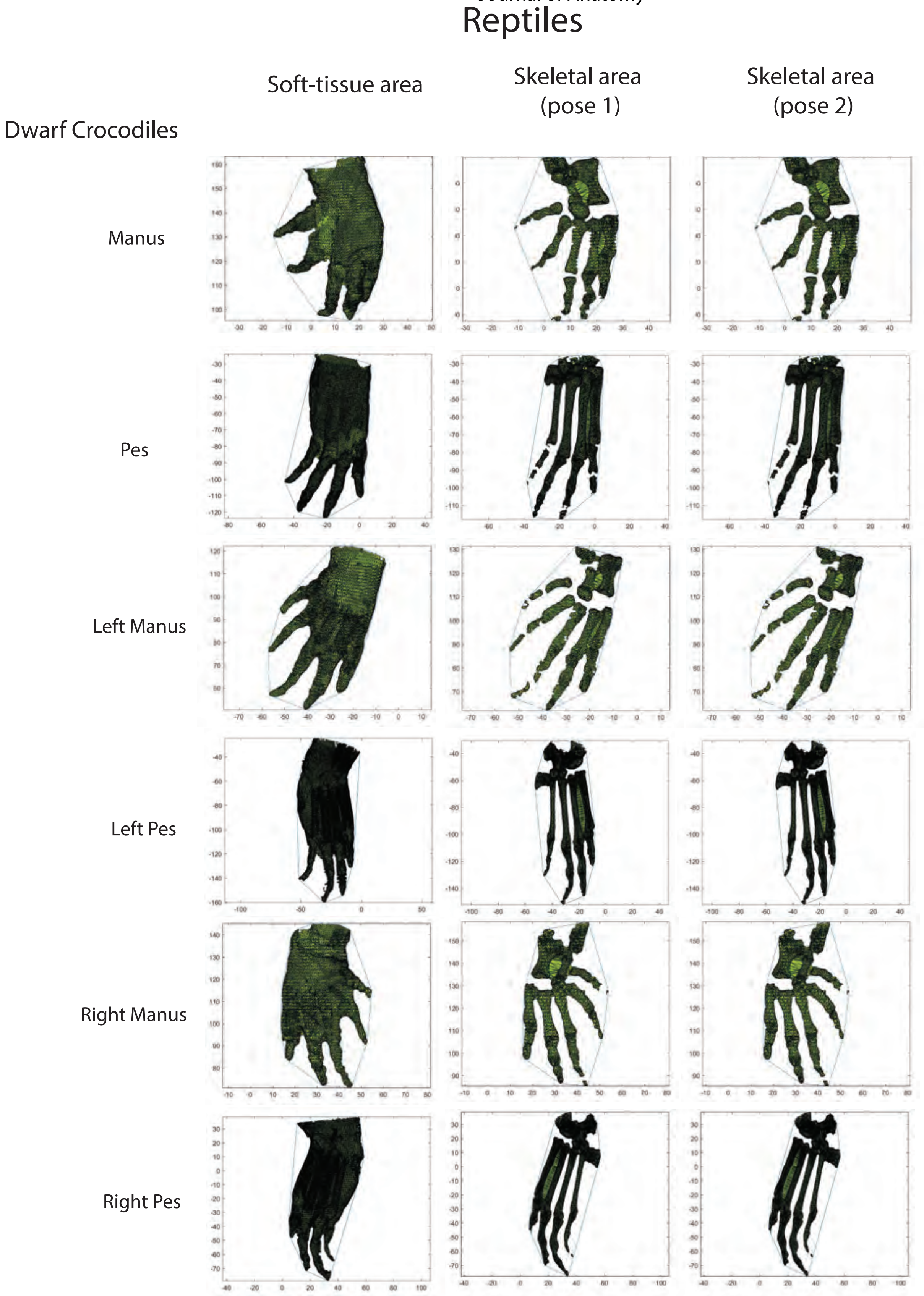
Reptiles
Soft-tissue area
Skeletal area (pose 1)
Skeletal area (pose 2)
Dwarf Crocodiles
Manus
Pes
Left Manus
Left Pes
Right Manus
Right Pes

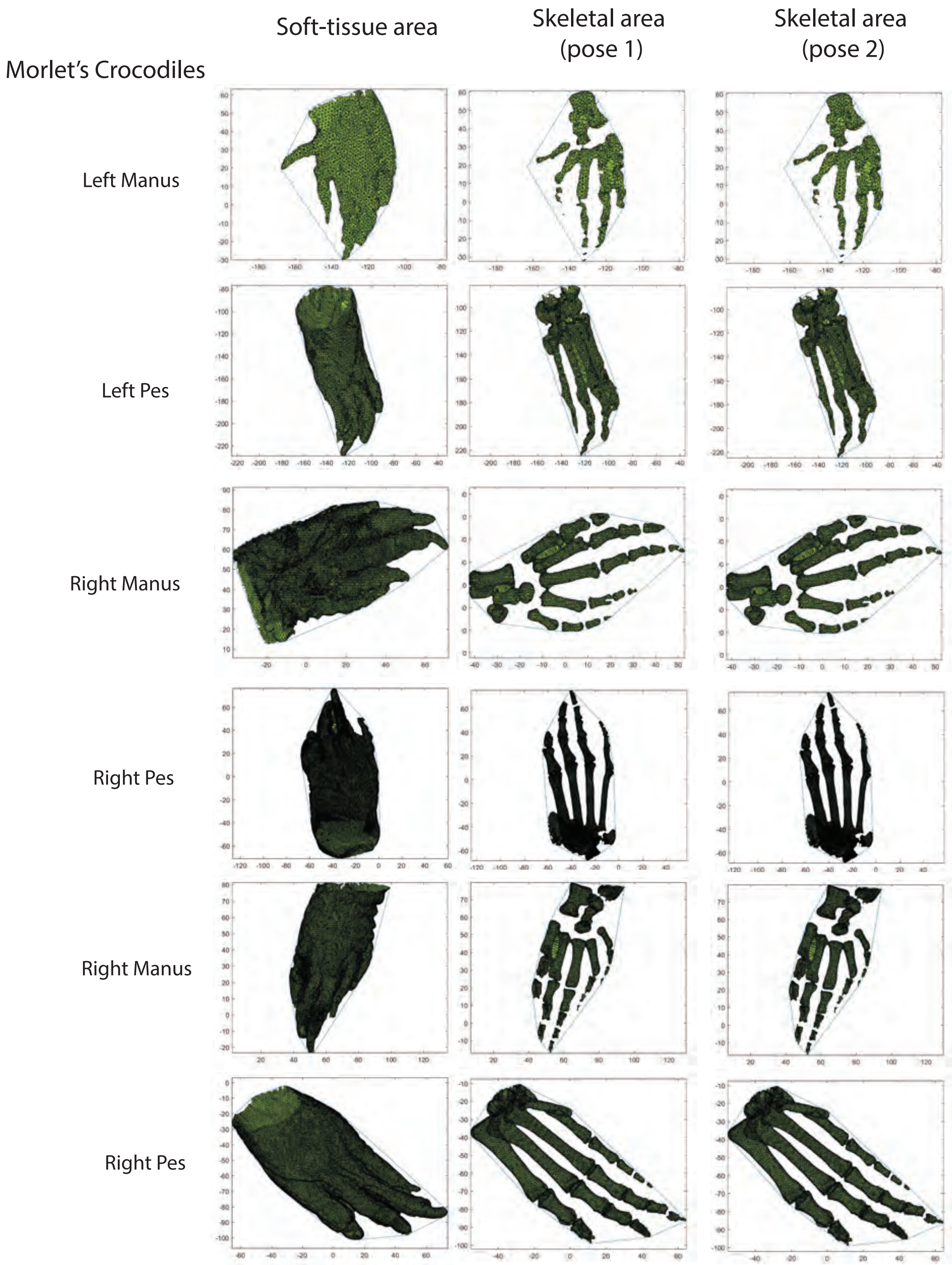
Soft-tissue area
Skeletal area (pose 1)
Skeletal area (pose 2)
Morlet's Crocodiles
Left Manus
Left Pes
Right Manus
Right Pes
Right Manus
Right Pes

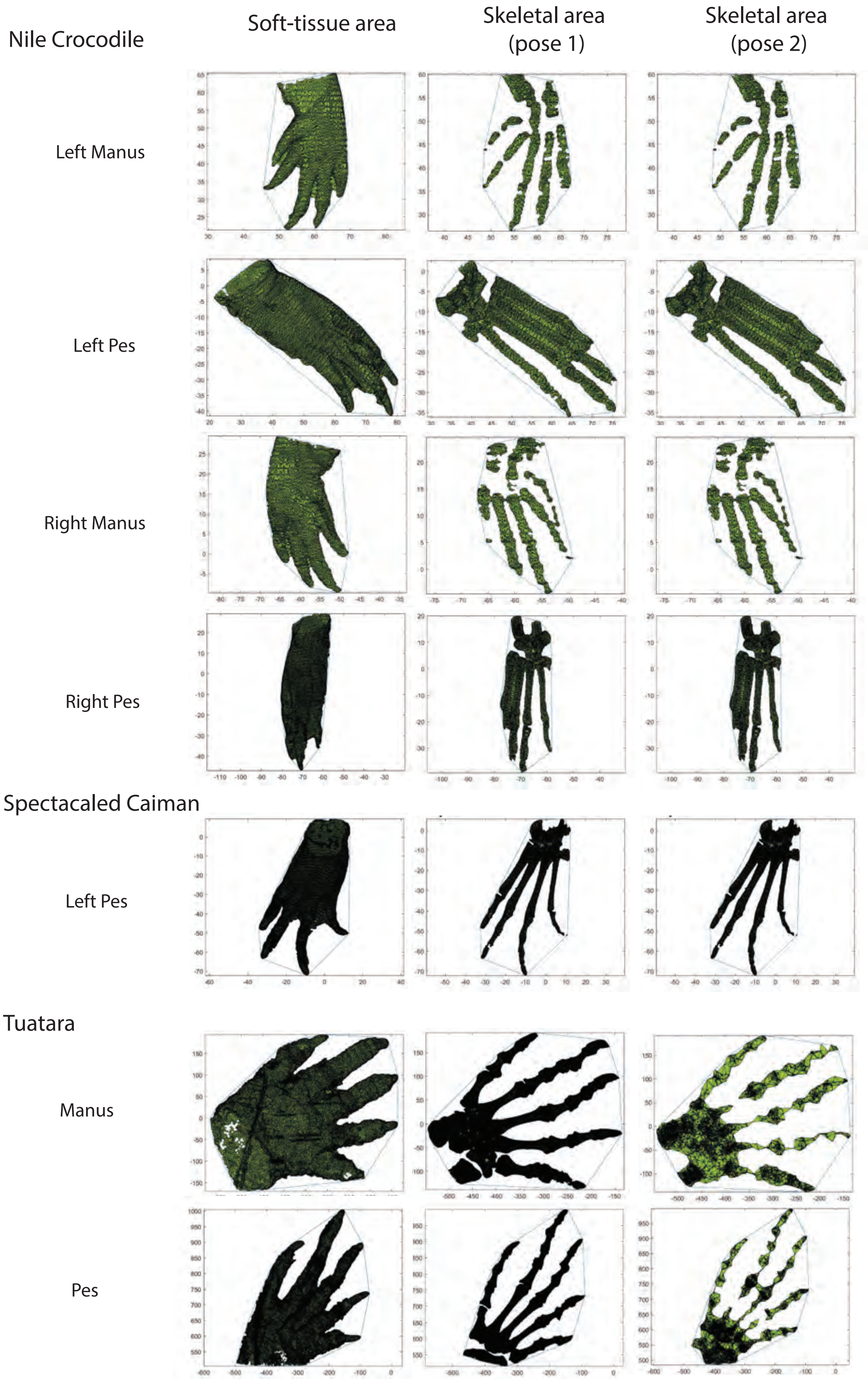
Nile Crocodile
Soft-tissue area
Skeletal area (pose 1)
Skeletal area (pose 2)
Left Manus
Left Pes
Right Manus
Right Pes
Spectacaled Caiman
Left Pes
Tuatara
Manus
Pes

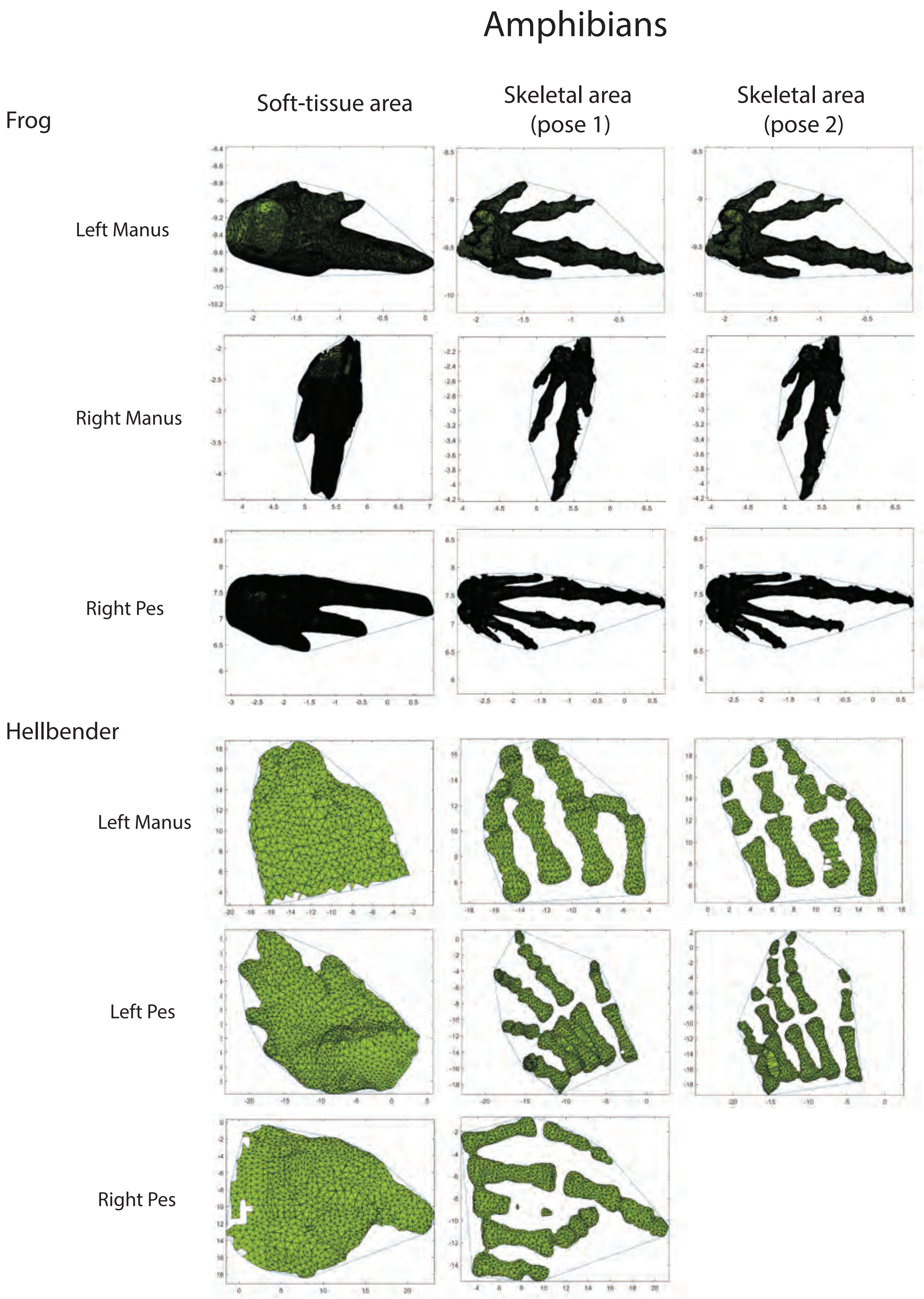
Amphibians
Frog
Soft-tissue area
Skeletal area (pose 1)
Skeletal area (pose 2)
Left Manus
Right Manus
Right Pes
Hellbender
Left Manus
Left Pes
Right Pes

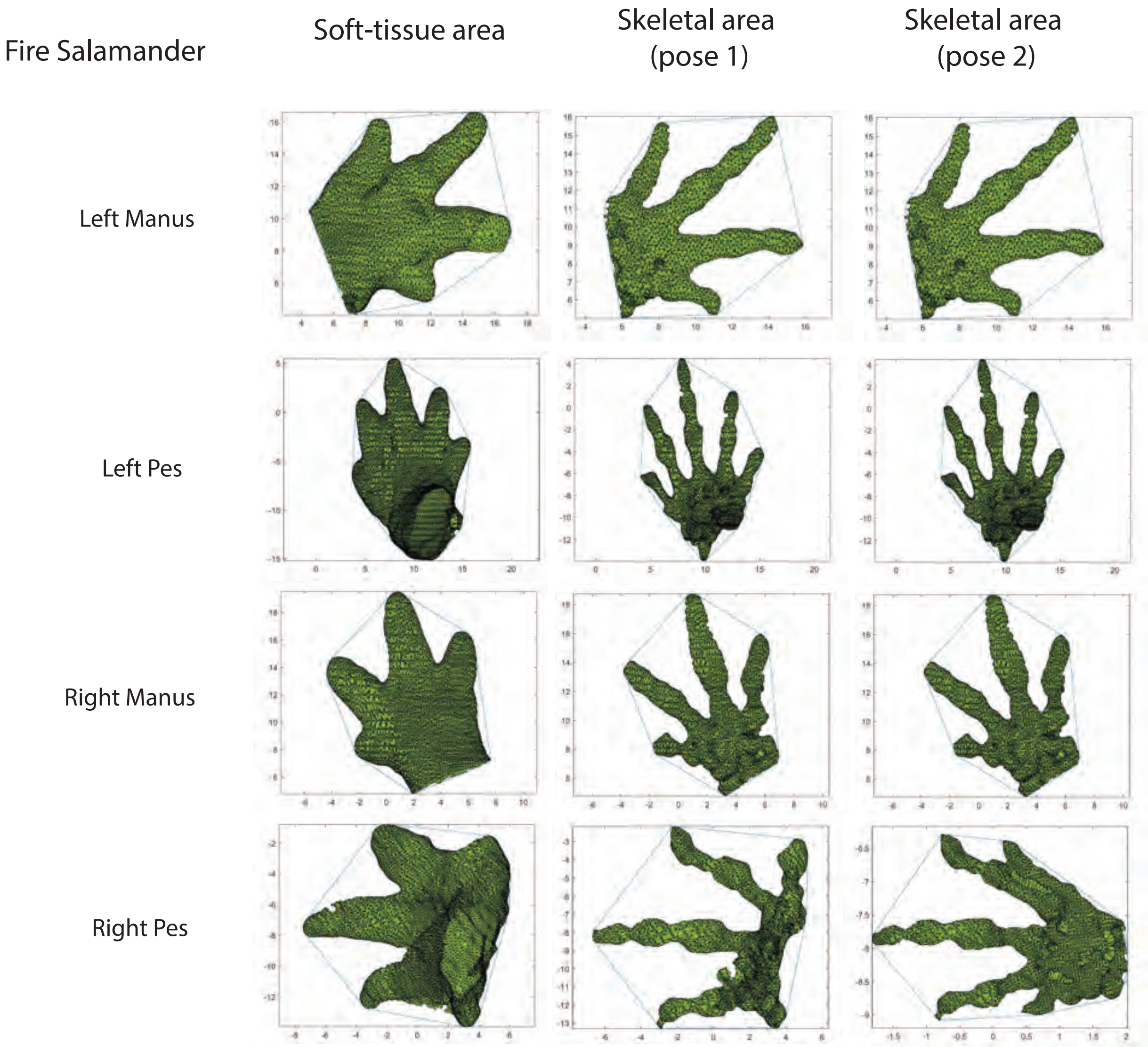
Fire Salamander
Soft-tissue area
Skeletal area (pose 1)
Skeletal area (pose 2)
Left Manus
Left Pes
Right Manus
Right Pes

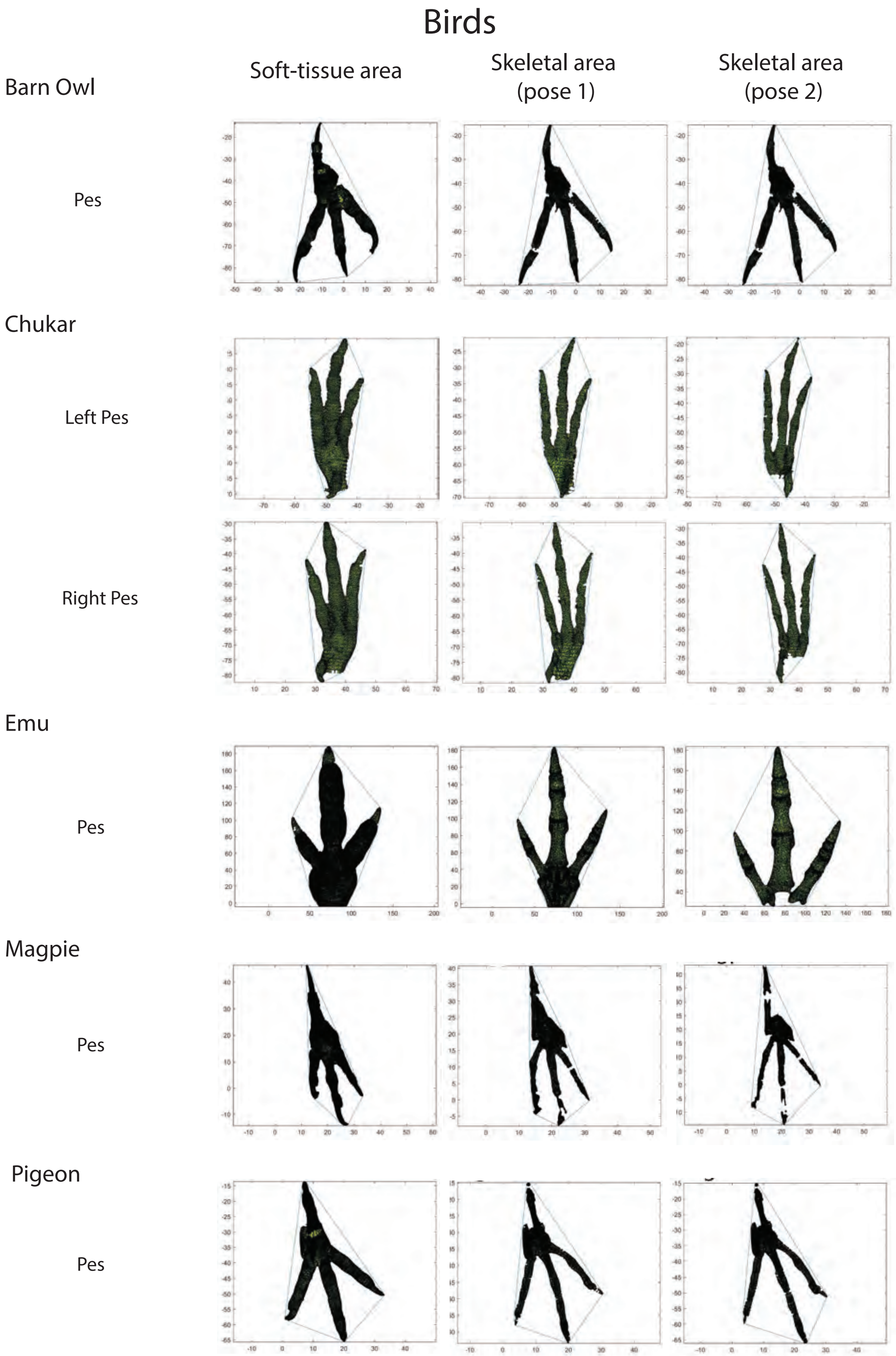
Birds
Soft-tissue area
Skeletal area (pose 1)
Skeletal area (pose 2)
Barn Owl
Pes
Chukar
Left Pes
Right Pes
Emu
Pes
Magpie
Pes
Pigeon
Pes

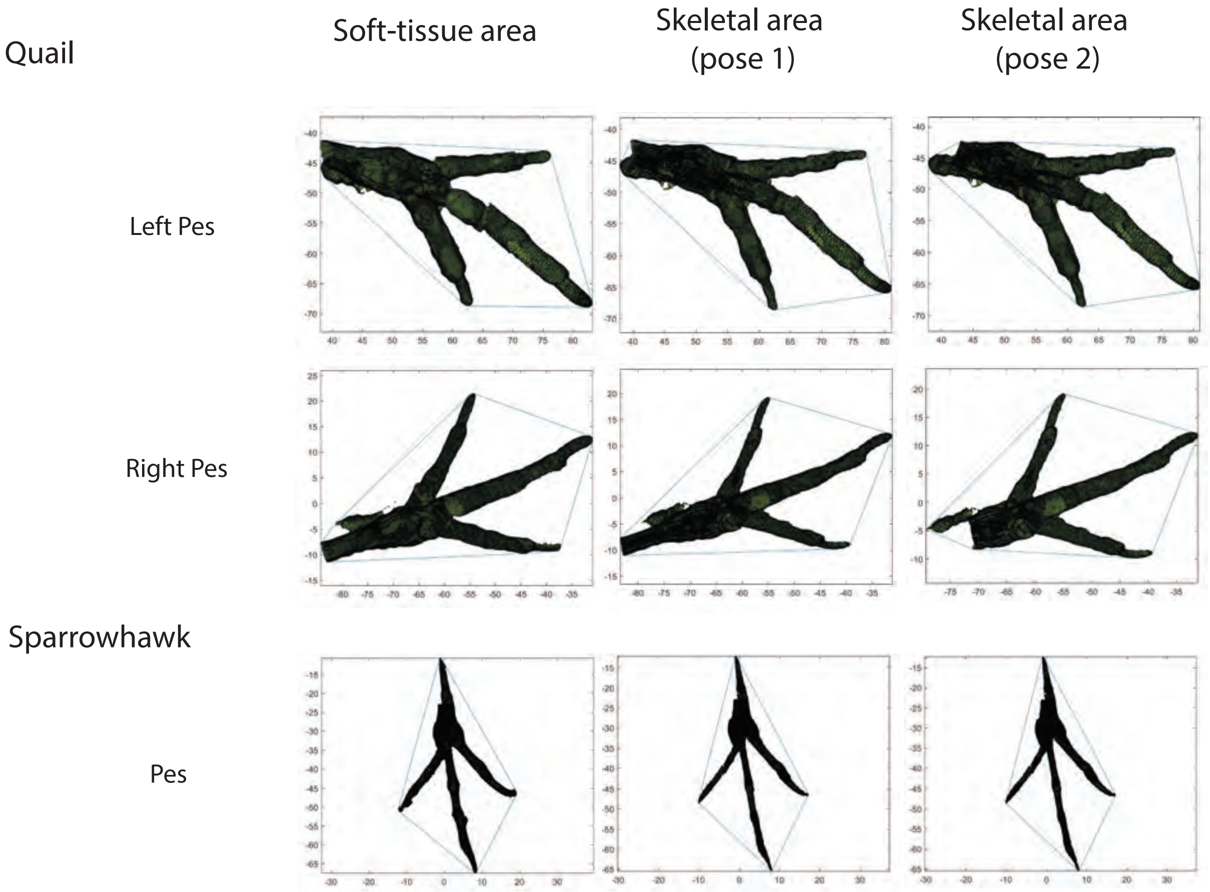
Quail
Soft-tissue area
Skeletal area (pose 1)
Skeletal area (pose 2)
Left Pes
Right Pes
Sparrowhawk
Pes